TECHNICAL MEMORANDUM

224

Impact of prognostic cloud scheme and subgrid scale orography on the simulation of the Asian summer monsoon

S. Das, M. Miller and P. Viterbo

Research Department

December 1995

European Centre for Medium-Range Weather Forecasts
Europäisches Zentrum für mittelfristige Wettervorhersage
Centre européen pour les prévisions météorologiques à moyen

Abstract

A new version of the ECMWF model CY13R4 was implemented on 4 April, 1995. This version includes a new prognostic cloud scheme, a smoothed mean orography with a new parametrization of the subgrid scale orography and changes in the numerics involving the semi-Lagrangian scheme. The performance of this version of the model was studied against the earlier version CY12R1 for 10 day forecasts, each from the initial conditions of 1-20 June of Monsoon-1994. Results indicated that both versions of the model were unable to predict many pockets of widespread convective rainfall over India. The mean of the 20 forecasts indicated that the CY12R1 underestimated rainfall over the Western Ghat, while CY13R4 overestimated the rainfall. The later version produced improved bias, RMSE and correlation coefficients with respect to observations of total cloudiness and 2 metre temperature as compared to the previous version. However, the RMSE of the predicted tracks of the cyclonic storm/monsoon depression were smaller for CY12R1 than for CY13R4. Similar results were also obtained from the operational version of the model for Monsoon-1995.

Sensitivity studies have been carried out to see the impact of subgrid scale orography and prescribed soil moisture on the rainfall over India. Results indicate that the new parametrization of SSO allows more convergence and cloudiness downstream away from the mountain. Experiments with prescribed initial wet and dry soil moisture values could not provide the solution to the failure of the model in predicting cases of widespread convective rainfall over the south Indian peninsula.

1. INTRODUCTION

The Asian summer monsoon is a well known feature of the general circulation of the atmosphere. Despite its regular seasonal cycle, the medium-range forecasts of its different characteristics such as the onset phenomenon, northward progress of the rainfall bands and genesis and movement of the monsoon depressions/cyclonic storms have been far from reality. The prediction of weather elements averaged over a longer duration of time such as monthly or seasonal features may look alright, but the real ability of a model could be justified only when it is able to predict extreme weather events properly in the medium-range time scale. In spite of a significant improvement in the forecast skills of the ECMWF model in recent years due to several reasons such as increased horizontal and vertical resolutions (*Ritchie et al*, 1995), improved parametrization of physical processes such as deep and shallow cumulus convection (*Tiedtke et al*, 1989), improved radiation parametrization (*Morcrette*, 1990) and land-surface processes (*Viterbo and Beljaars*, 1995), the model performance in the tropics still lags behind that in the extratropics.

Three major changes were introduced in ECMWF's operational model in April, 1995; (i) a new prognostic cloud scheme, (ii) smoothed mean orography with a new parametrization of the subgrid scale orography and (iii) changes in the numerics involving the semi-Lagrangian scheme and some other minor changes. When tested independently, these changes have respectively been shown to provide better cloud cover and cloud water contents (*Tiedtke*, 1993), a better estimate of the mountain drag, flow dynamics and low level wake observed in mesoscale analysis (*Lott and Miller*, 1995) and controlled aliasing arising from quadratic terms over poles in the reduced gaussian grid (*Courtier and Naughton*, 1994). The purpose of this paper is to assess the performance of the new version of the model, in particular with regard to the Asian summer monsoon. In the context of the following discussions it will be assumed that the changes in the semi-Lagrangian scheme do not significantly impact on the phenomena being considered. A few sensitivity studies have been carried out to understand the problem of underprediction of widespread convective rainfall over the Indian region.

Section 2 briefly describes the changes made in the model. In Section 3, we present a comparison of the CY13R4 versus CY12R1. The performance of the operational model during monsoon-1995 is discussed in Section 4. Section 5 describes the sensitivity experiments and, finally, conclusions are presented in Section 6.

2. DESCRIPTION OF RECENT CHANGES IN THE MODEL

Detailed descriptions of these changes have been described in their respective papers as mentioned in the introduction. However, for completeness, we shall briefly describe here the two major changes made in the model.

2.1 The prognostic cloud scheme

The new cloud scheme was developed by *Tiedtke* (1993) and implemented in ECMWF's Integrated Forecasting System (IFS) by *Jakob* (1994). In this scheme, the time evolution of cloud cover and cloud water content is determined by two additional prognostic equations which include their sources and sinks due to diabatic processes as follows

$$\frac{\partial l}{\partial t} = A(l) + S(l)_{CV} + S(l)_{BL} + C - E - G_p - \frac{1}{\rho}\frac{\partial}{\partial z}(\rho\overline{\omega' l'})_{Entr} \qquad (1)$$

$$\frac{\partial a}{\partial t} = A(a) + S(a)_{CV} + S(a)_{BL} + S(a)_C - D(a) \qquad (2)$$

where 'l' is the liquid water content and 'a' is the cloud cover. The terms denoted by $A(\ )$ represent advective transport (not implemented in the current operational version), while the terms denoted by $S(\ )_{CV}$, $S(\ )_{BL}$ represent the sources due to convection and boundary layer processes respectively. C is the condensation/sublimation rate and E is the rate of evaporation of cloud water/ice. G_p is the rate of generation of precipitation by conversion of cloud drops into raindrops and deposition of cloud ice. The last term in equation (1) is the flux divergence due to entrainment process at the top of stratocumulus clouds and the term $D(a)$ in equation (2) is the rate of decrease of cloud area due to evaporation. Clouds are thus allowed to form due to boundary layer processes, horizontal transport of liquid water detrained from cumulus tops, large scale ascent and diabatic cooling. They dissipate through turbulent mixing of cloud with environment, adiabatic and diabatic heating and depletion of cloud water by precipitation. Cloud microphysical processes in warm and mixed water/ice clouds are parametrized following *Sundquist* (1988), while for ice clouds the method of *Heymsfield and Donner* (1990) has been used.

The new cloud scheme has several advantages over the diagnostic scheme in terms of better physical description of the hydrological cycle through coupling of the cloud scheme to model's convection scheme. It has shown better simulation of global cloudiness, precipitation characteristics and time evolution of anvil and cirrus clouds. However, there are several uncertainties involved in the new cloud scheme, such as the separation of the total condensate in the cloud water and cloud ice which are presently distinguished depending on temperature, but may in the future be treated separately using prognostic equations for water and ice content. Deficiencies have also been noted in the representation of stratocumulus clouds over extratropics. There is observational evidence that, in the tropics, shallow and deep convective clouds can coexist (*Yanai et al*, 1976; *Das et al*, 1987) which are not allowed in the present version of the model.

2.2 The Subgrid Scale Orography parametrization

Since 1983, the ECMWF model orography was created at every model resolution by adding an increment proportional to the standard deviation of the subgrid scale orography to the mean orography over the grid box.

This so called "envelope orography" was introduced in order to parametrize the mountain blocking effects on the atmospheric flow and, at the time of introduction, produced significant reductions of the systematic errors. Nevertheless, there were at least two major disadvantages of using an envelop orography: (a) it is a flow independent way of parametrizing mountain effects, (b) it is detrimental to the data assimilation system since a significant fraction of the low level data (around 15% of the SYNOPS) is rejected due to the inconsistencies between the envelope orography and the station height.

In the new scheme, drag is parametrized in a flow dependent way on model levels which are intersected by the subgrid scale orography. The SSO over a grid point is represented by four parameters which are standard deviation, anisotropy, slope of orography and the geographical location of the orography. In this scheme the low level wind is partitioned into two parts. The first part corresponds to the incident flow which passes over the mountain top while the second part is the blocked flow for which the blocking height Z_b is the highest level located below the mountain top for which the flow change between Z_b and the mountain top exceeds a critical value F_c. The scheme was first used in an off-line calibration where the SSO was used to predict the mountain pressure drag and vertical profiles of the momentum fluxes and the results were compared with the observations collected over the Pyrenees during PYREX. The T213 forecasts with this scheme showed that the forecast mountain drag consistently reproduced the drag measured during PYREX.

3. COMPARISON OF CY13R4 VS CY12R1

A re-assimilation of the data was carried out with the new version of the model for the period 1-20 June, 1994. Ten day forecasts were made from each of the twenty initial conditions. In this section, we shall first discuss the comparison of the weather elements; rainfall, clouds and 2 metre temperature. We shall then study the forecast errors of the track of a cyclonic storm which formed during the period and finally discuss the scores of geopotential and wind vectors.

3.1 **Weather elements**

The Root Mean Square Errors (RMSE), Bias and Correlation Coefficients of rainfall, total cloudiness and 2 metre temperature above the ground were computed for the 10 day forecasts obtained from the initial conditions of 1-20 June, 1994. These statistics were computed with respect to the observed station values over the Indian region as well as over Europe. The results are described below.

3.1.1 *Rainfall*

Figure 1 shows the observed and 72 hour predicted rainfall based on the initial condition of June 3, 1994 which was obtained from the two versions of the model. The monsoon had progressed up to Goa by 6 June, 1994 which is depicted in the forecasts of both models. However, the diagrams show that there are many pockets

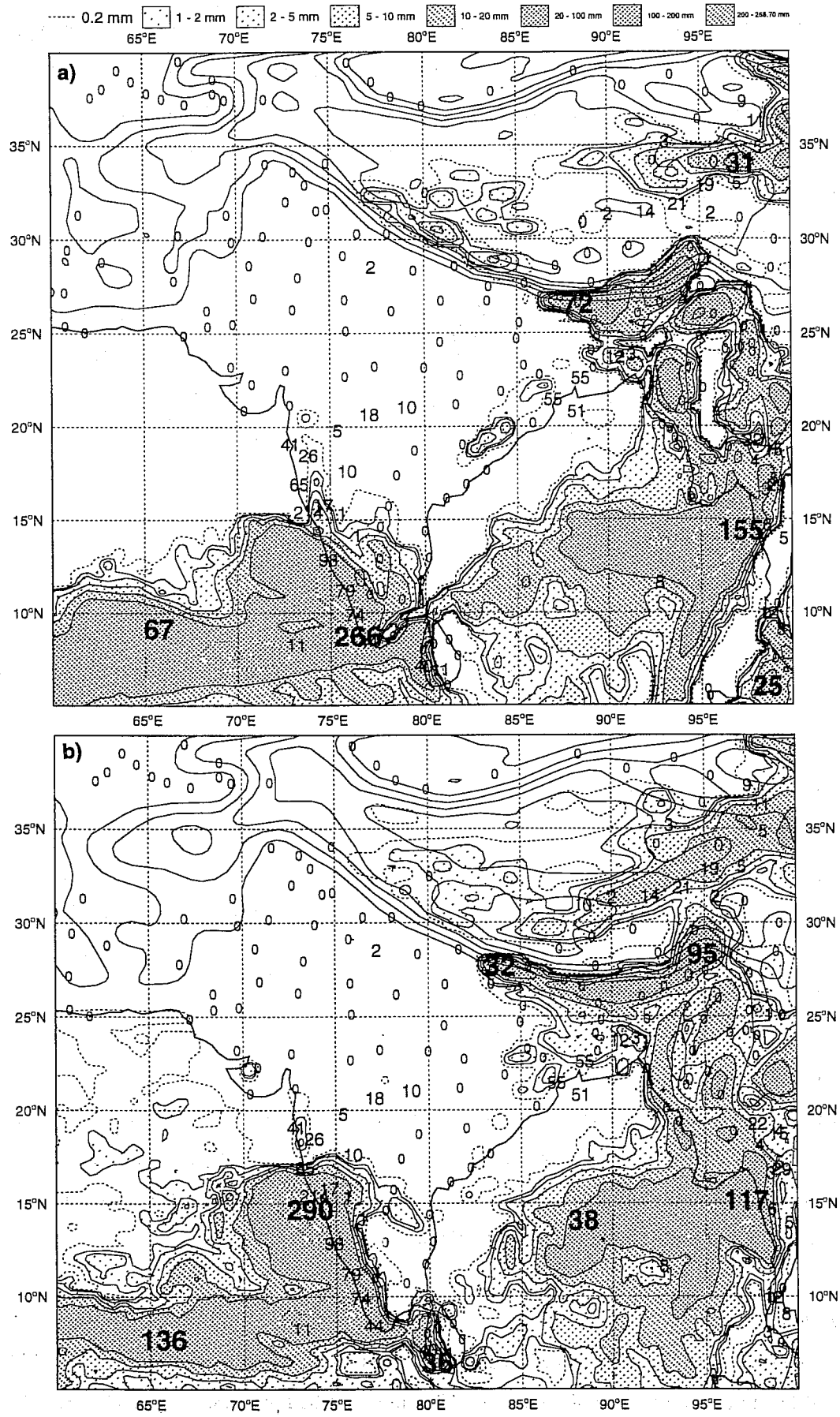

Fig 1 72 hour rainfall predicted from the initial condition of 12UTC, 3 June, 1994 by (a) Cy12 R1 and (b) CY13R4.

of convective rainfall over Maharastra and coastal Orissa which were not predicted by any of the models. The CY13R4 forecast was relatively better, but similar weakness of the model was found on many occasions of the pre-monsoon season when the model was unable to predict many areas of wide spread convective rainfall.

Fig 2 shows the mean distribution of errors in 72 hours rainfall forecasts obtained from the two cycles during 1-20 June, 1994. Comparison of the two versions indicates that the CY12R1 (upper diagram) underestimates rainfall over most of the places including the Western-Ghat. On the other hand, the CY13R4 overestimates rainfall over the Ghat mountains and underestimates over most of the central and southern peninsular India. It is not clear at this stage what is the cause of the overestimation of the rainfall over the Western-Ghat.

Fig 3 depicts the Bias, RMSE and Correlation Coefficients of a series of daily cumulative rainfall forecasts for 10 days and averaged for the period 1-20 June, 1995. These statistics were obtained with respect to the observations at the synoptic stations. The left panel shows the values averaged over the Indian region (5-40° N, 60-100° E). For comparison, the right panel shows the values averaged over Europe (25-60° N, 18° W-70° E). Comparison of the two versions indicate that the CY13R4 has a larger positive bias and higher RMSE as compared to the previous cycle over the Indian region. Comparison of the results between India and Europe indicate that both versions are able to forecast better precipitation over Europe than compared to the Indian region.

3.1.2 *Clouds*

Fig 4 shows the mean distribution of errors for 72 hours forecasts of total cloudiness averaged over the period 1-20 June, 1994 as obtained from the two versions. It indicates that CY12R1 underestimated the total cloudiness over most parts of India while the new version produced much better distribution of the clouds. The time series of mean Bias, RMSE and Correlation Coefficients for 5 day forecasts of the total cloudiness are shown in Fig 5. The left, middle and the right panels illustrate average over the Indian region (0-40° N, 60-100° E), Europe (25-60° N, 18° W-70° E) and Tropics (30° S-30° N). Results indicate that the new version produced better cloudiness over all three regions. Comparison of forecasts over the three regions indicates that the correlation coefficient falls below 60% after two days over Europe. The general performance of cloudiness forecasts appears to be better over India than compared to the whole tropics and Europe. This may be due to the persistent large cloud amounts present over the Indian region during the monsoon season. In other words, the performance is relatively poor where the variability of cloudiness with respect to time is larger such as over Europe or over the entire tropics during this season. Deficiencies have also been noted in the CY13R4 in capturing the shallow cumulus clouds over the land.

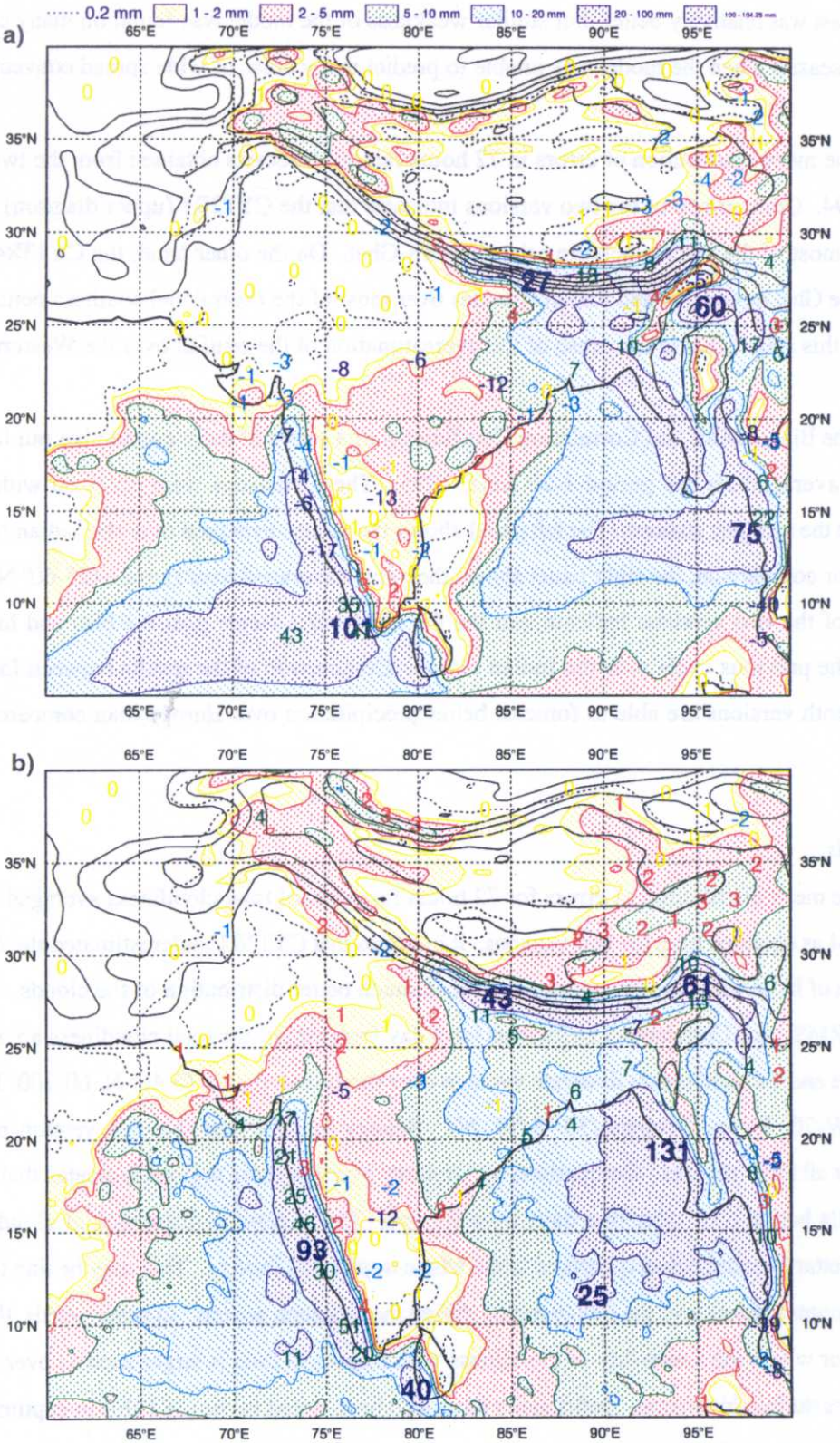

Fig 2 Mean 72 hours forecast errors of total precipitation for the period 1-20 June, 1994 obtained from (a) CY12R1 and (b) CY13R4.

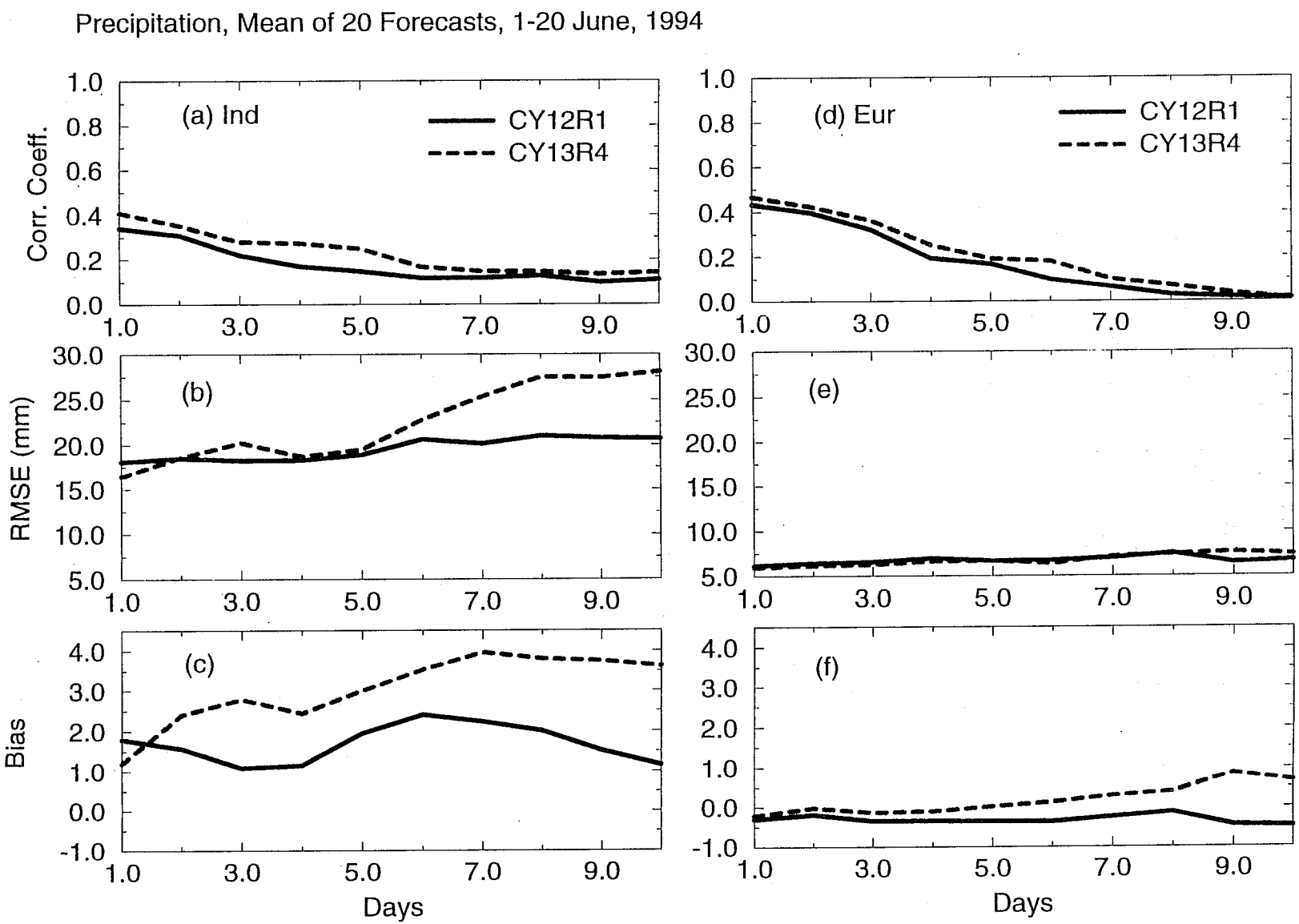

Fig 3 Time series of 10 days forecast mean Bias, RMSE and Correlation Coefficients of total precipitation for the period 1-20 June, 1994 over the Indian region and Europe obtained from CY12R1 and Cy13R4.

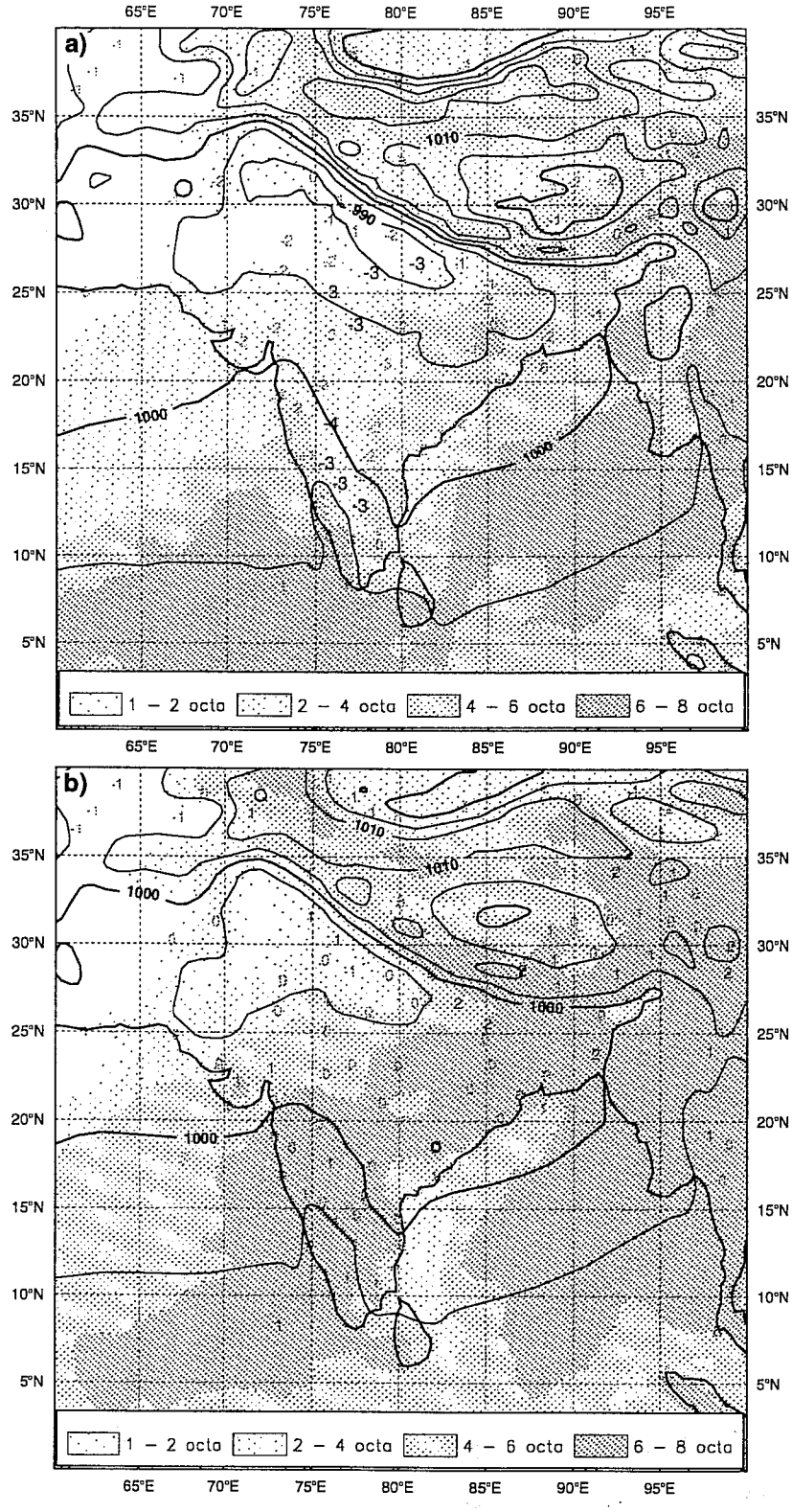

Fig 4 As in fig 2 but for the total cloudiness obtained from (a) CY12R1 and (b) CY13R4.

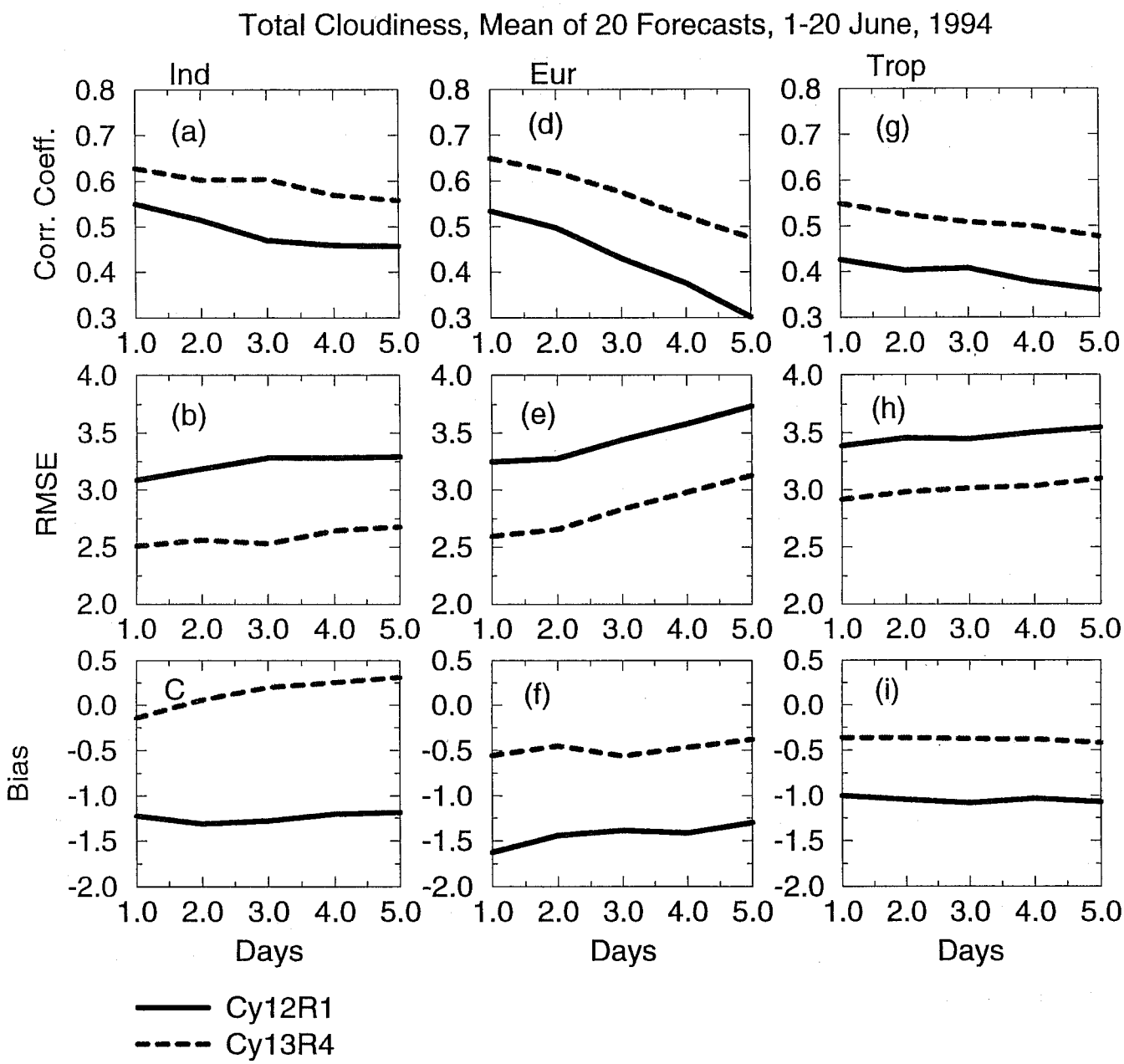

Fig 5 As in Fig 3 but for the Total Cloudiness.

Figures 6 and 7 show the 72 hour forecasts of the total, high, middle and low cloudiness averaged for the period 1-20 June, 1994 obtained from the two versions of the model. Comparison of the two diagrams indicates that the new version produced better distribution of total cloudiness since the monsoon had covered most parts of the west, central and north-eastern India by that time. There are two maxima of the high clouds as expected produced from the deep cumulus convection over the Western-Ghat, north-east India and adjoining the Bay of Bengal during this time. The diagrams indicate that the distribution of these clouds is better produced by the new cloud scheme than compared to the old one. The amounts of middle and low clouds are much higher in the new scheme than compared to the old scheme. Moreover, the CY13R4 shows more structures in the horizontal distributions of clouds.

Figure 8 illustrates the 72 hour forecasts of the OLR averaged over the period 1-20 June, 1994. The upper panel is for the CY13R4 while the lower panel shows the difference between CY13R4 and CY12R1. Two minima of the OLR are seen, one associated with the deep clouds over the Western-Ghat and another over the Arakan coast. The maximum OLR over northwest India and adjoining Pakistan where the clouds are relatively less and shallow at this time is reasonably well produced by the model. The difference field shown in the lower diagram indicates that the new scheme produced higher clouds over the Western-Ghat and the Arakan coast as compared to the old scheme.

3.1.3 *Temperature at 2 metres*

Figure 9 shows the mean errors of the 72 hour forecasts of the temperature at 2 metres above the ground as obtained from the two versions of the models. The diagrams indicate that the old model had a tendency to produce very warm surface temperatures due to the lack of cloudiness during day time. This has been remarkably improved by the new version due to better forecasts of the total cloudiness. The 5 day forecast time series of mean bias, RMSE and correlation coefficients of the 2 metre temperature obtained from the two versions of the models is depicted in Fig 10. The statistics were obtained by using the observed station values from the GTS data. The left, middle and right panels show the values averaged over the Indian region, Europe and the Tropics respectively. The diagrams clearly show that the 2 metre temperatures predicted by the new model compare better with the observations. Comparison of the three regions indicates that there is much less variation in the scores over the tropics which is perhaps due to less diurnal variability of surface temperature in most parts of this region during this time.

3.2 **Cyclonic storm/depression**

In this section we shall describe the comparison of the two versions of the model in forecasting the tracks of cyclonic storms. A cyclonic storm formed off the west coast of India on 5 June, 1994. The storm initially moved towards northwest, carrying the monsoon up to Bombay, then towards west over the Arabian sea and finally weakened and lost its significance on 9 June. The upper part of Fig 11 illustrates (a) the tracks of this

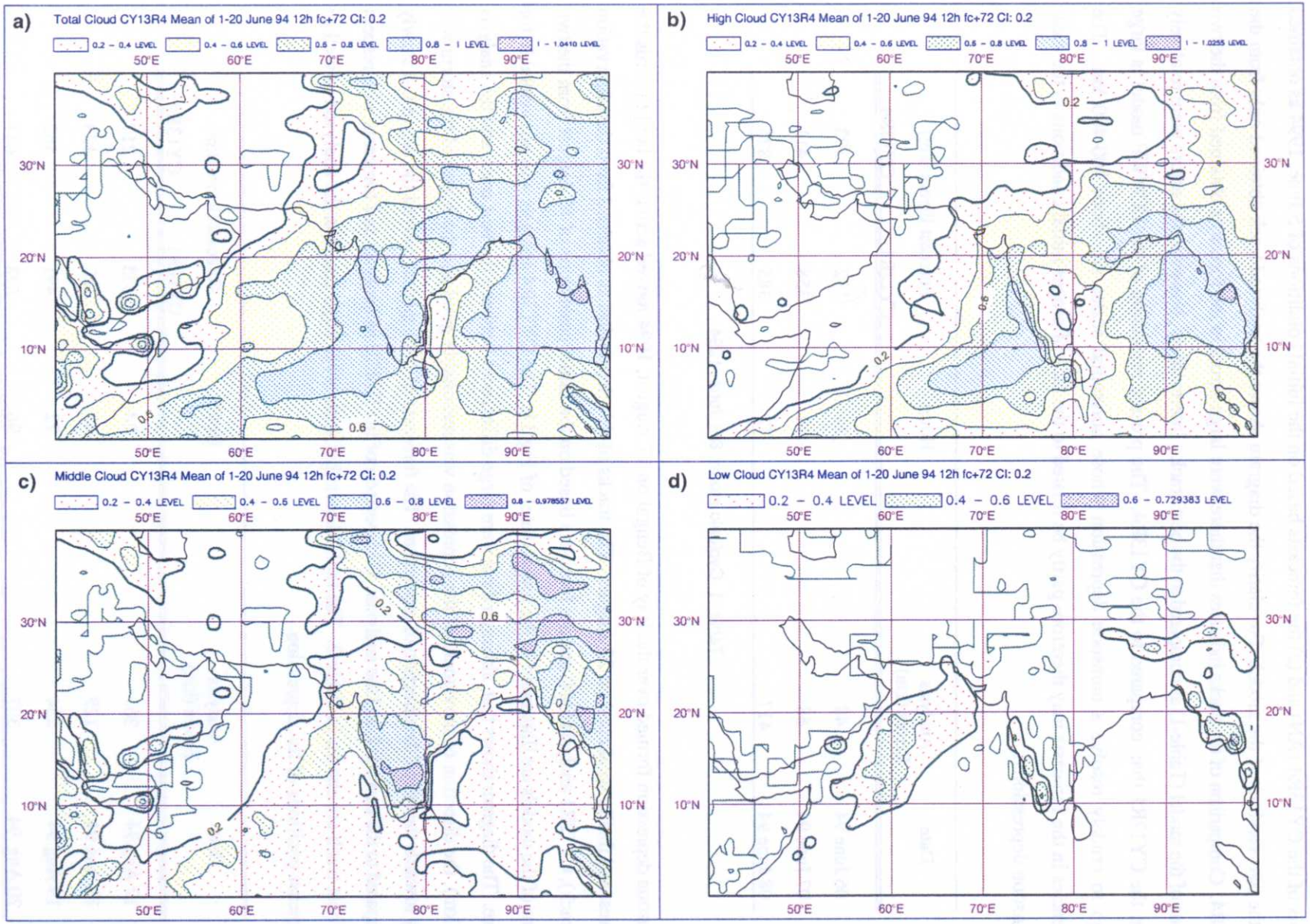

Fig 6 Mean of 72 hour forecasts over the period 1-20 June, 1994 obtained from the CY13R4 for (a) Total Cloudiness, (b) High Cloudiness (c) Middle cloudiness and (d) Low Cloudiness.

storm as obtained from the observations (Best Track) provided by the Indian Meteorological Department, (b) analysis of the CY13R4 (AN) and (c) the forecasts based on the initial conditions of 5 June, 1994 as obtained from the two versions of the model. For clarity the diagram shows the analysed track obtained only from the CY13R4. Comparison of the tracks indicates that there were large errors in the forecasts obtained from the two versions of the model (Table-1) as compared to the best track. Interestingly, however, the errors were relatively less in the CY12R1 than compared to the CY13R4. The present resolution of the ECMWF model is large enough to crudely resolve a monsoon depression whose horizontal scales are about 300-400 km. The deficiencies in the forecasts may therefore partly be related to the lack of proper initial conditions in the areas of monsoon depressions.

Date	Analysis Errors (km)	Hours	Forecast Errors (km)	
			CY12R1	CY13R4
06 June 94	48	24	192	193
07 June 94	68	48	358	411
08 June 94	417	72	385	875

Table: 1 Cyclonic storm, 6-8 June, 1994

A monsoon depression formed over the Bay of Bengal on 17 August, 1994 moved across the land towards the northwest and finally weakened on 20 August. The tracks of this depression as obtained from the observation (best track), CY12R1 analysis (AN) and the forecasts based on the initial conditions of 16 August from the two versions of the models are illustrated in the lower panel of Fig 11. The CY13R4 analysis was not available for this date. The diagram shows that, although there were large differences between the best track and the analysis (~250 km), the direction of movement of the depression was reasonably good and the centre of the storm was usually towards the left of the direction of movement. The forecasts of both models moved the storm too slowly as compared to the best track and the analysis. Comparison of the RMSE of analysis and forecasts with respect to the best track are shown in Table 2. The table shows that there were large errors in the analysed as well as the forecast positions of the depression.

Date	Analysis Errors (km)	Hours	Forecast Errors (km)	
			CY12R1	CY13R4
17 Aug 94	201	24	233	217
18 Aug 94	129	48	85	123
19 Aug 94	234	72	491	562
20 Aug 94	307	96	698	641

Table: 2 Monsoon depression, 17-20 August, 1994

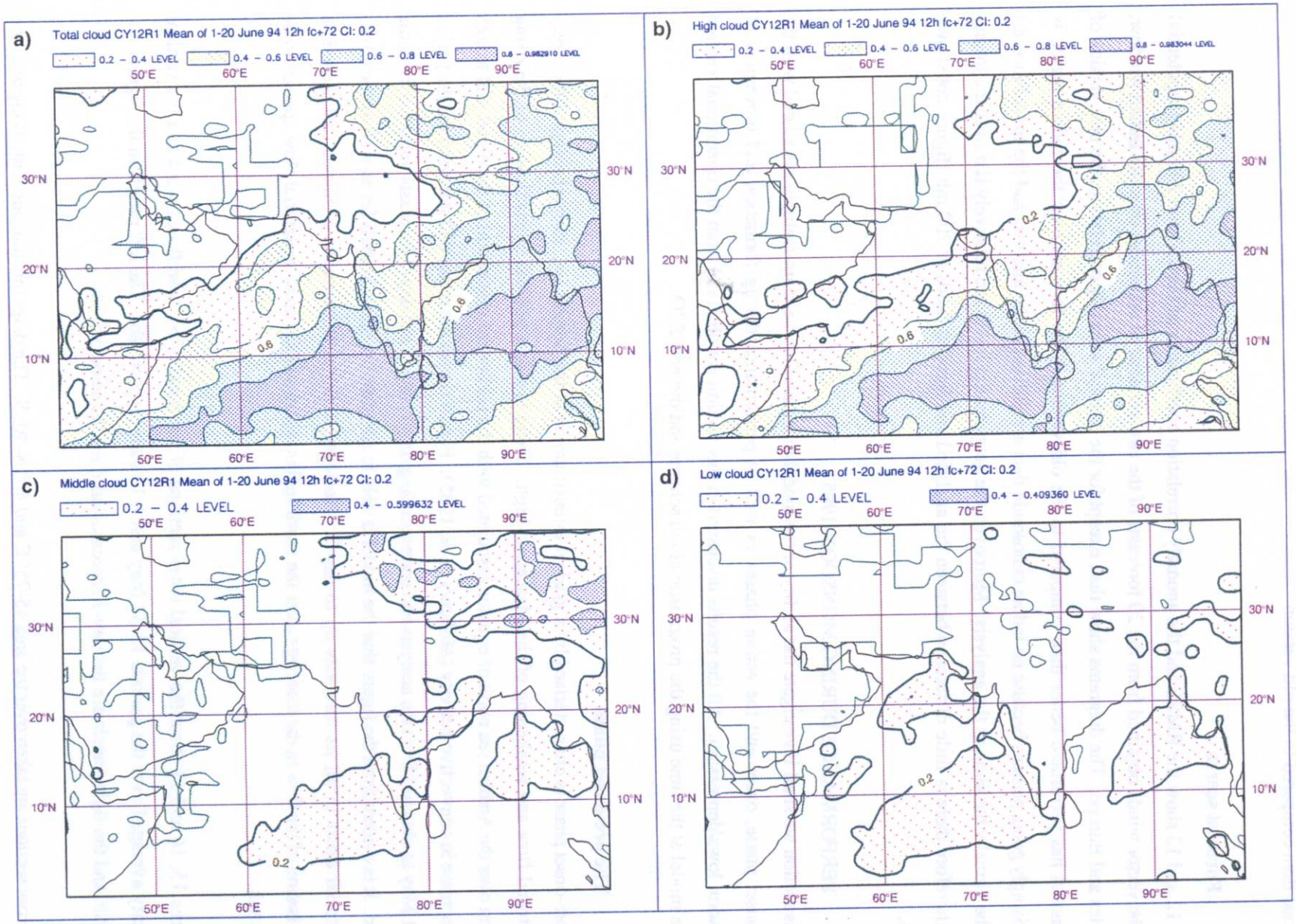

Fig 7 As in fig 6 but for CY12R1.

Results are mixed but the rainfall values (not shown here) showed relatively better distribution in the CY13R4 forecast than compared to the old version.

3.3 **Forecast scores**

Figs 12 and 13 show the RMSE and the anomaly correlation coefficients of the 850 and 200 mb geopotential and the vector winds obtained from the 20 forecasts of the two versions of the model over the Indian window, Tropics and Europe. The diagrams show that, except for the tropical anomaly correlation, the new version of the model has performed better than compared to the old version. The forecast over the Indian region is surprisingly good, perhaps because no Indian radiosonde data are utilised in the analysis and the model forecast may be virtually the same as the analysis. Moreover, the geopotential levels are relatively flat over the tropics and therefore there is little difference between the analysed and forecast fields at 200 mb (figure not shown here).

4. PERFORMANCE DURING MONSOON-1995

In this section we shall investigate the ability of the model in simulating the main features associated with the pre-onset phase, onset and the active phases as well as performance during formation and movement of monsoon lows/depression. All the results discussed in this section are obtained from the operational version of the model at the time using the prognostic cloud scheme and the new SSO.

4.1 **The pre-onset phase**

The pre-onset phase is characterised by a gradual intensification of the Somali Jet, strengthening of the cross-equatorial flow and weakening of the Mascerean high. There is also a gradual intensification of the rising motion over the Arabian sea north of equator associated with the northward movement of the equatorial trough and increase in convective activity (*Mohanty et al*, 1985). Fig 14 shows the mean 850 mb wind for the period 15-31 May as obtained from the analysis and corresponding day-1, day-3 and day-7 forecasts valid for the same period. It is evident from the figure that the model is able to simulate the mean Somali Jet as well as the cross-equatorial flows in all its forecasts up to day-7. However, a closer examination indicates that there is a zonalisation of the flow in the forecasts over the north Indian ocean and the cross equatorial flow appears to be too weak.

Figures 15, 16 and 17 show the vertical cross sections of the zonal wind, meridional wind and the vertical velocity averaged over the periods 15-31 May and 1-15 June respectively. The left panels in the figures are analysis and the right panels are the day-7 forecasts valid for the same periods.

The cross sections are taken over the area 45-75° E and 40° N-40° S. The diagrams indicate that, along with the progress of the season, the low level westerlies over the Arabian sea north of the equator increase in strength

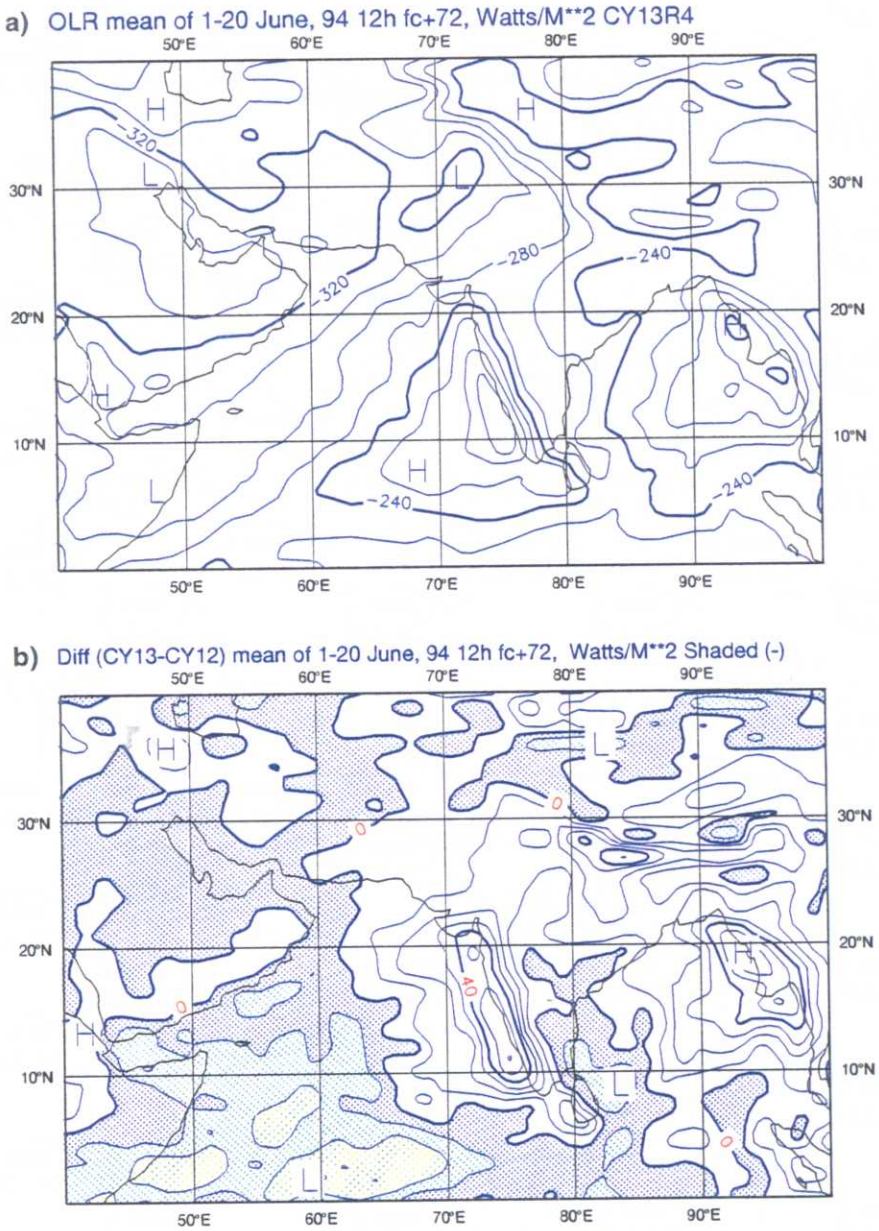

Fig 8 Mean of 72 hour forecasts of OLR over the period 1-20 June, 1994 obtained from (a) CY13R4 and (b) CY12R1.

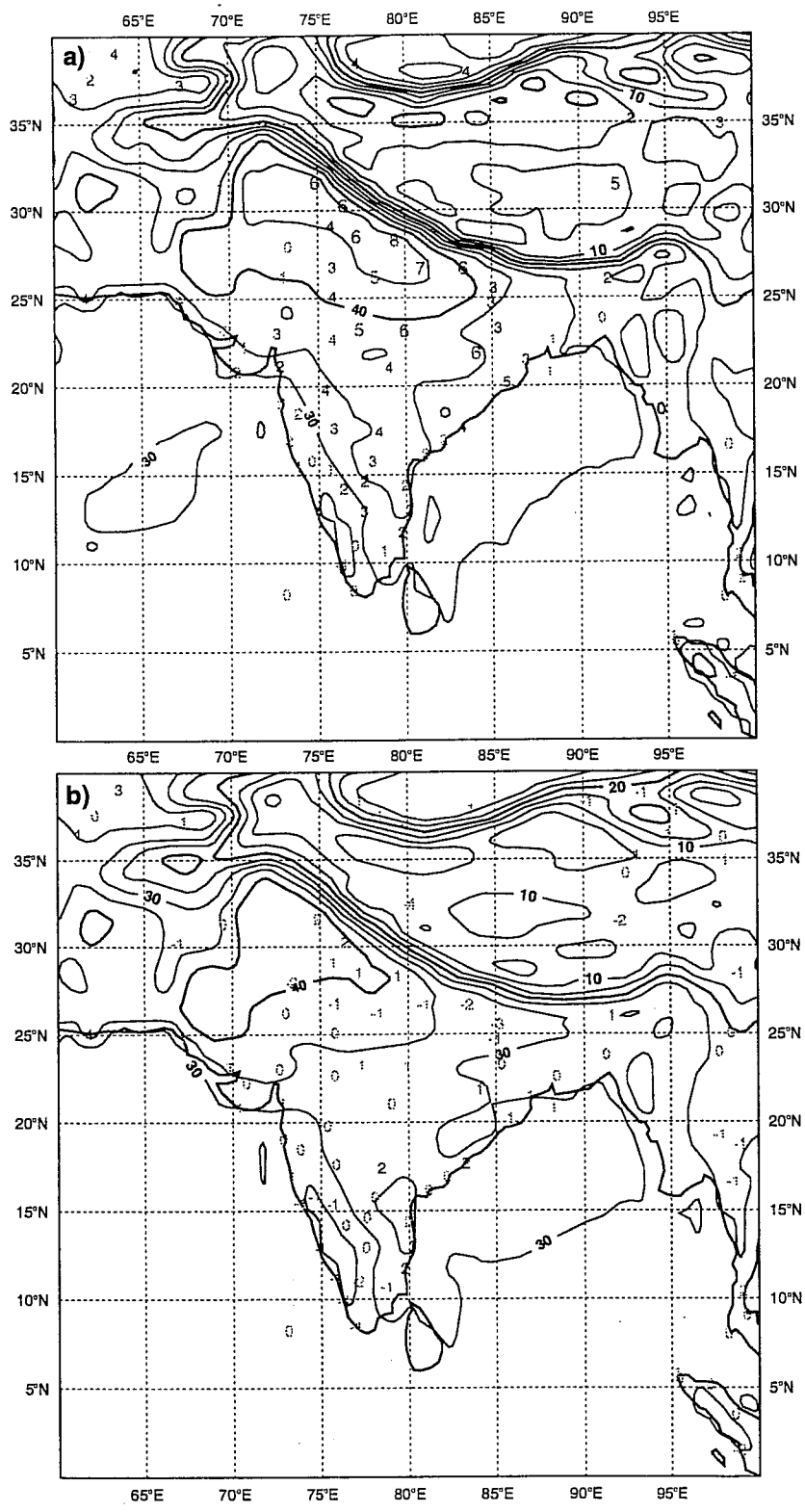

Fig 9 As in fig 2 but for the 2 metre temperature obtained from (a) CY12R1 and (b) CY13R4.

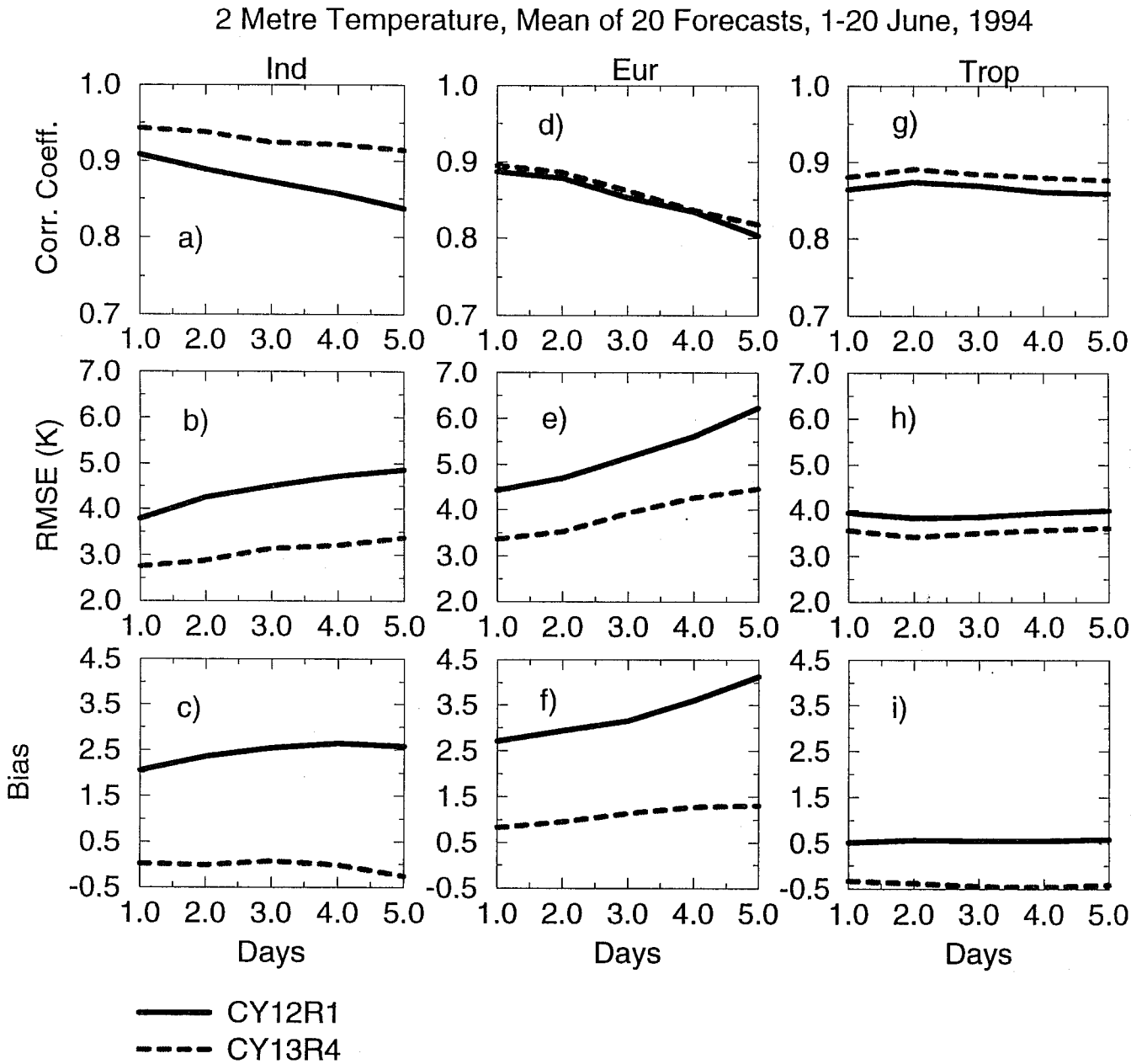

Fig 10 As in Fig 3 but for the 2 metre temperature.

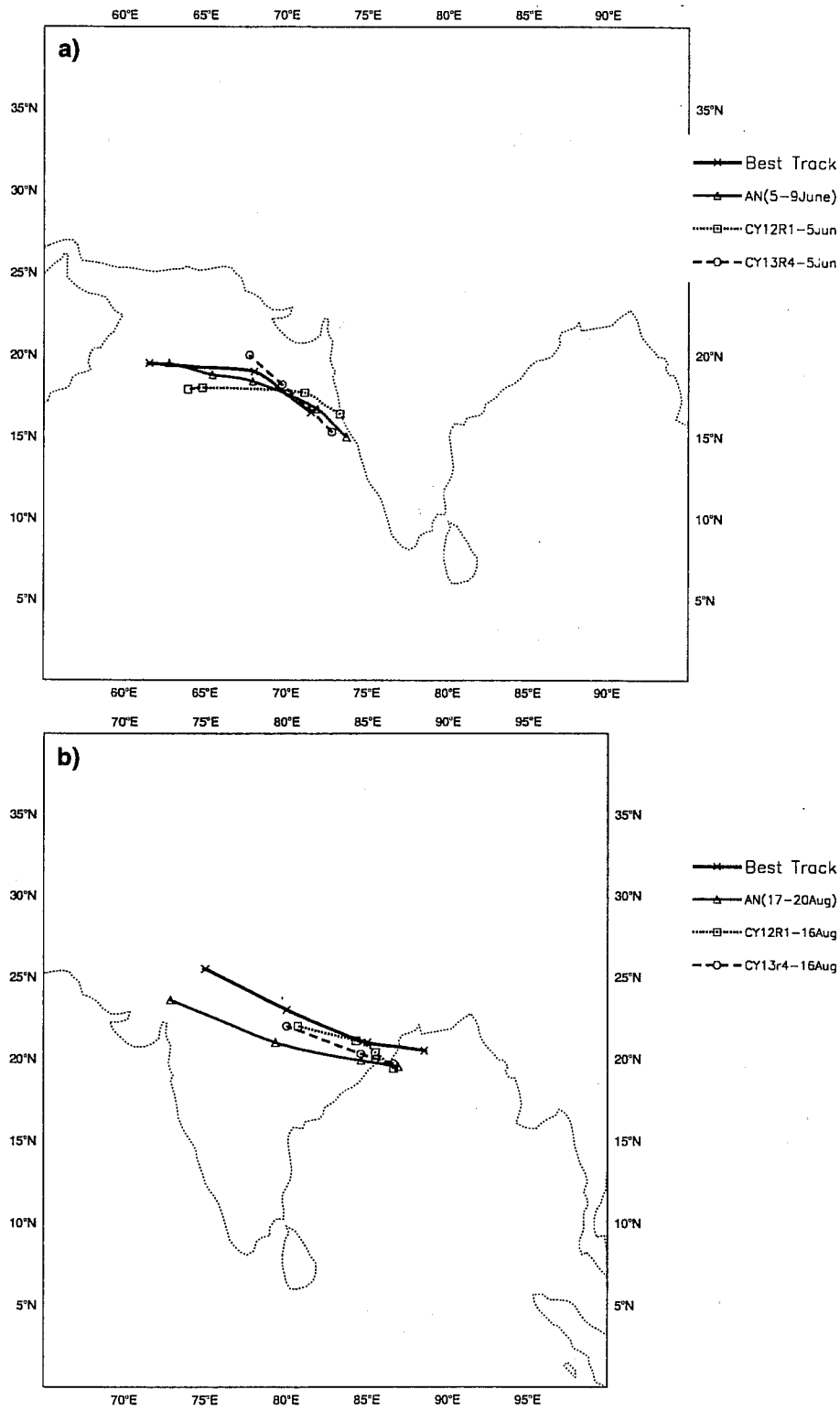

Fig 11 Observed, analysed and predicted tracks obtained from CY12R1 and CY13R4 for (a) the cyclonic storm of 5-9 June, 1994 and (b) Monsoon depression of 17-20 August, 1994.

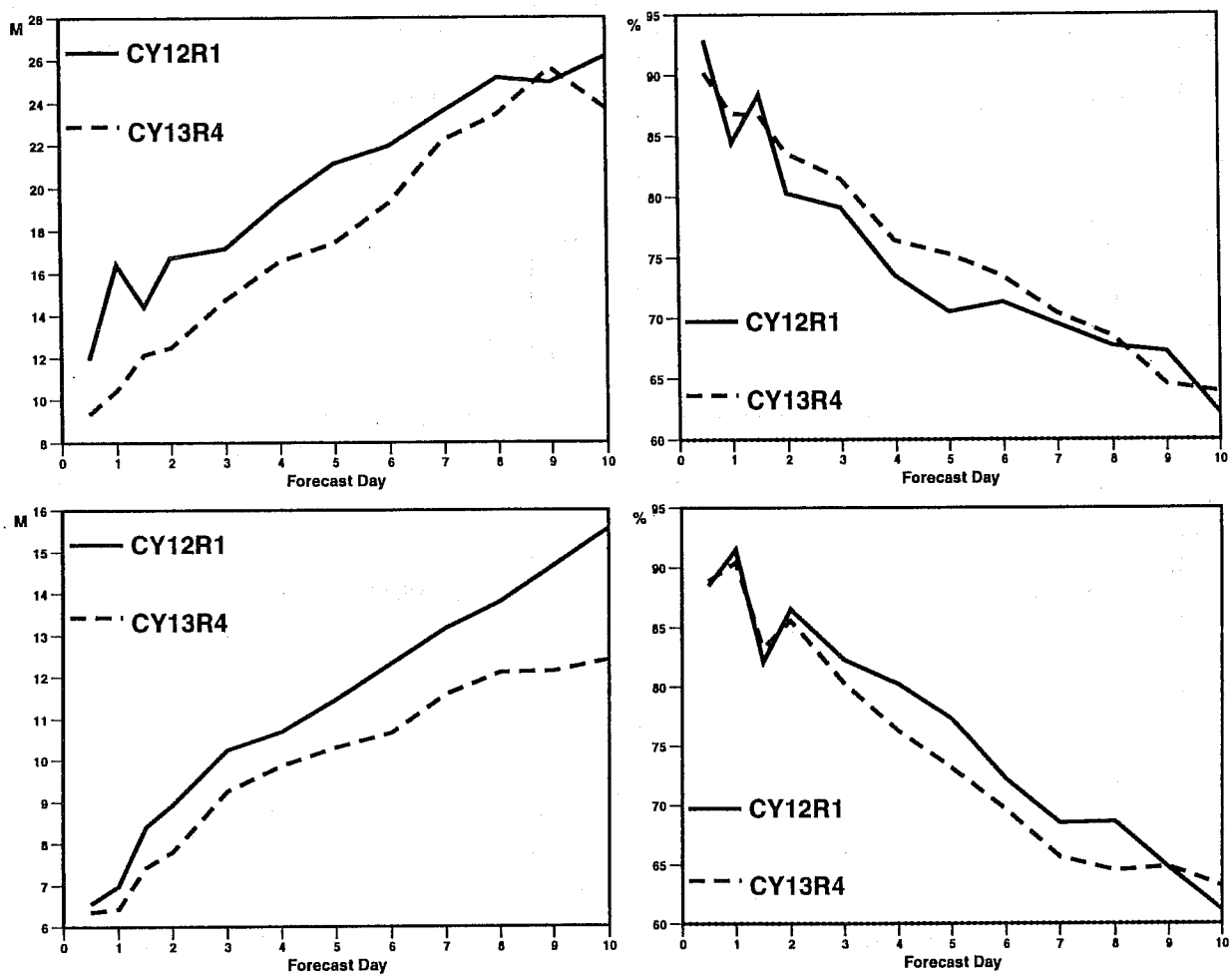

Fig 12 Root Mean Square and Anomaly Correlations of the 10 days forecasts of 850 mb Geopotential for the period 1-20 June, 1994 over the Indian region, and Tropics.

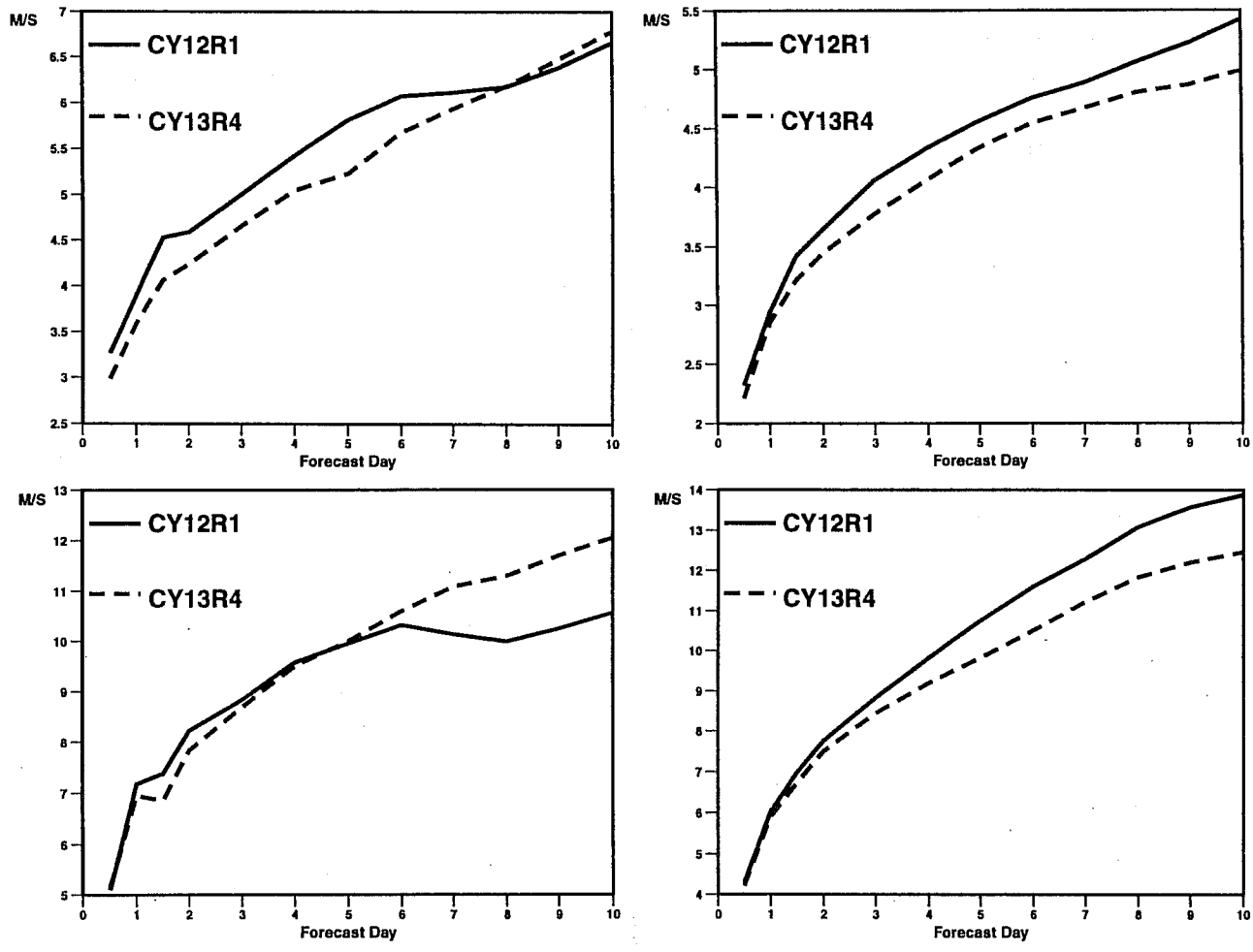

Fig 13 As in Fig 12 but for 850 and 200 mb wind vectors.

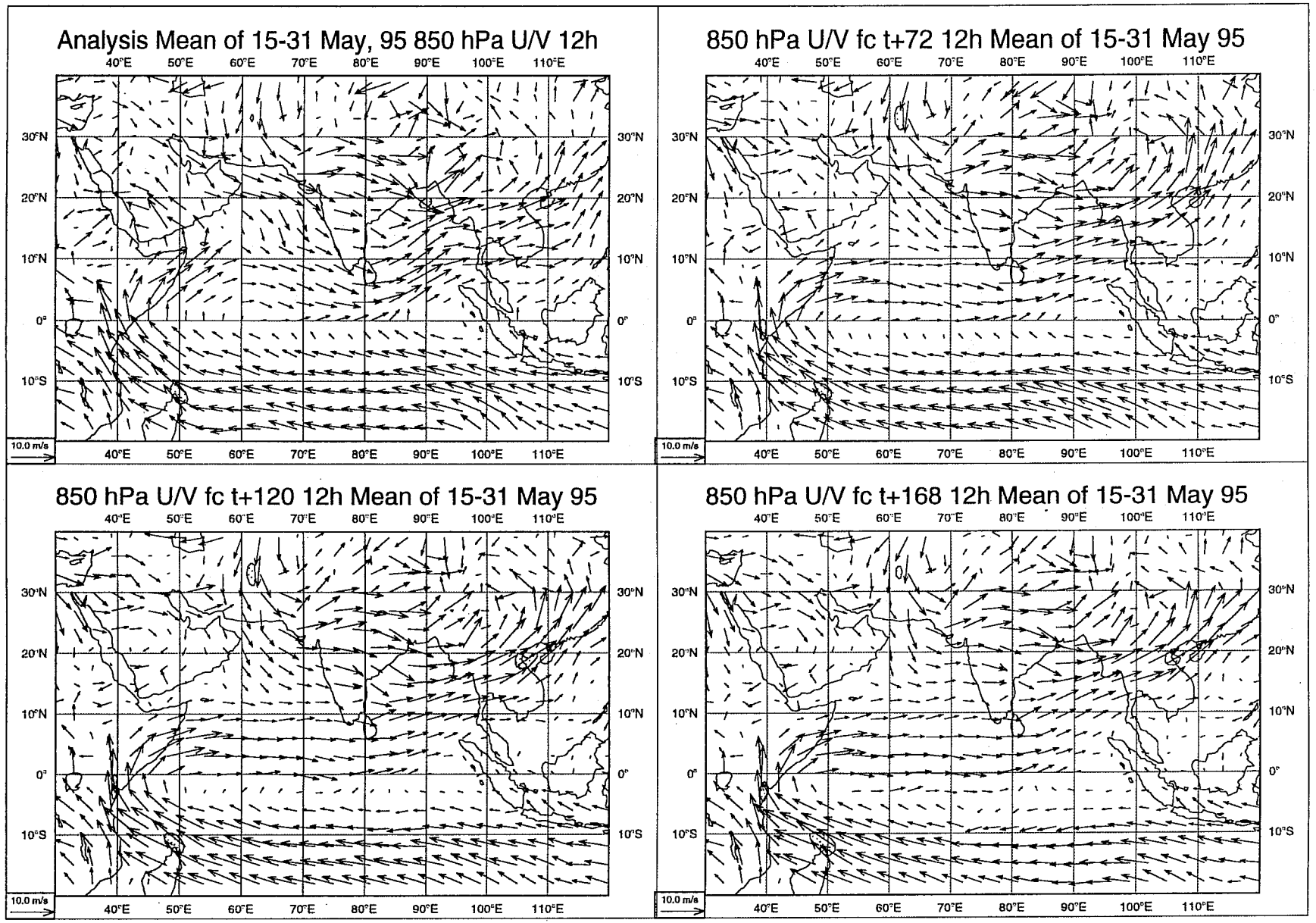

Fig 14 Mean of 850 mb wind Analysis, Day-3, Day-5 and Day-7 forecasts averaged over the period 15-31 May, 1995.

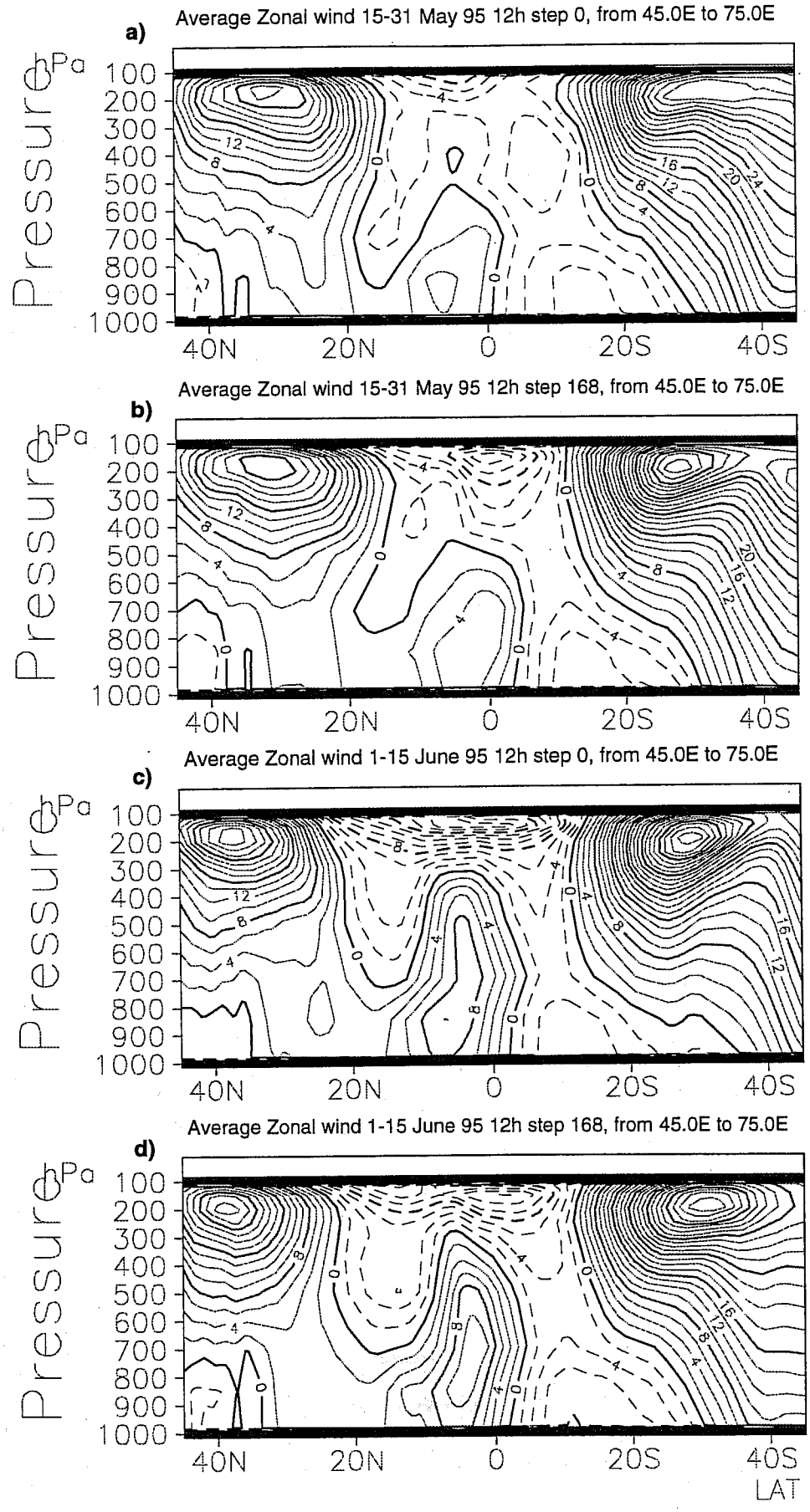

Fig 15 Vertical cross sections of mean zonal wind Analysis and Day-7 forecasts averaged over the periods 15-31 May and 1-15 June, 1995.

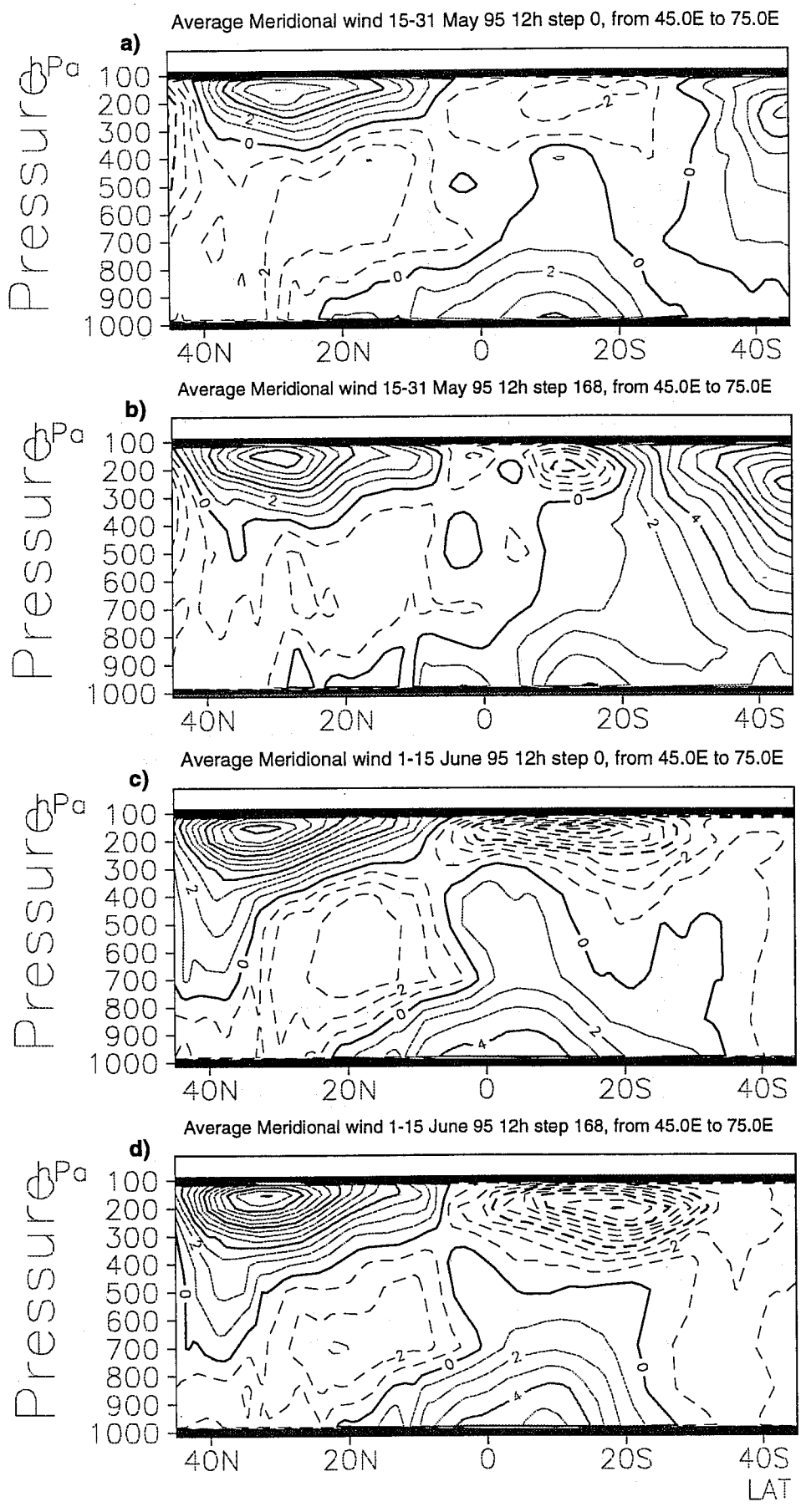

Fig 16 As in Fig 15 but for the meridional wind.

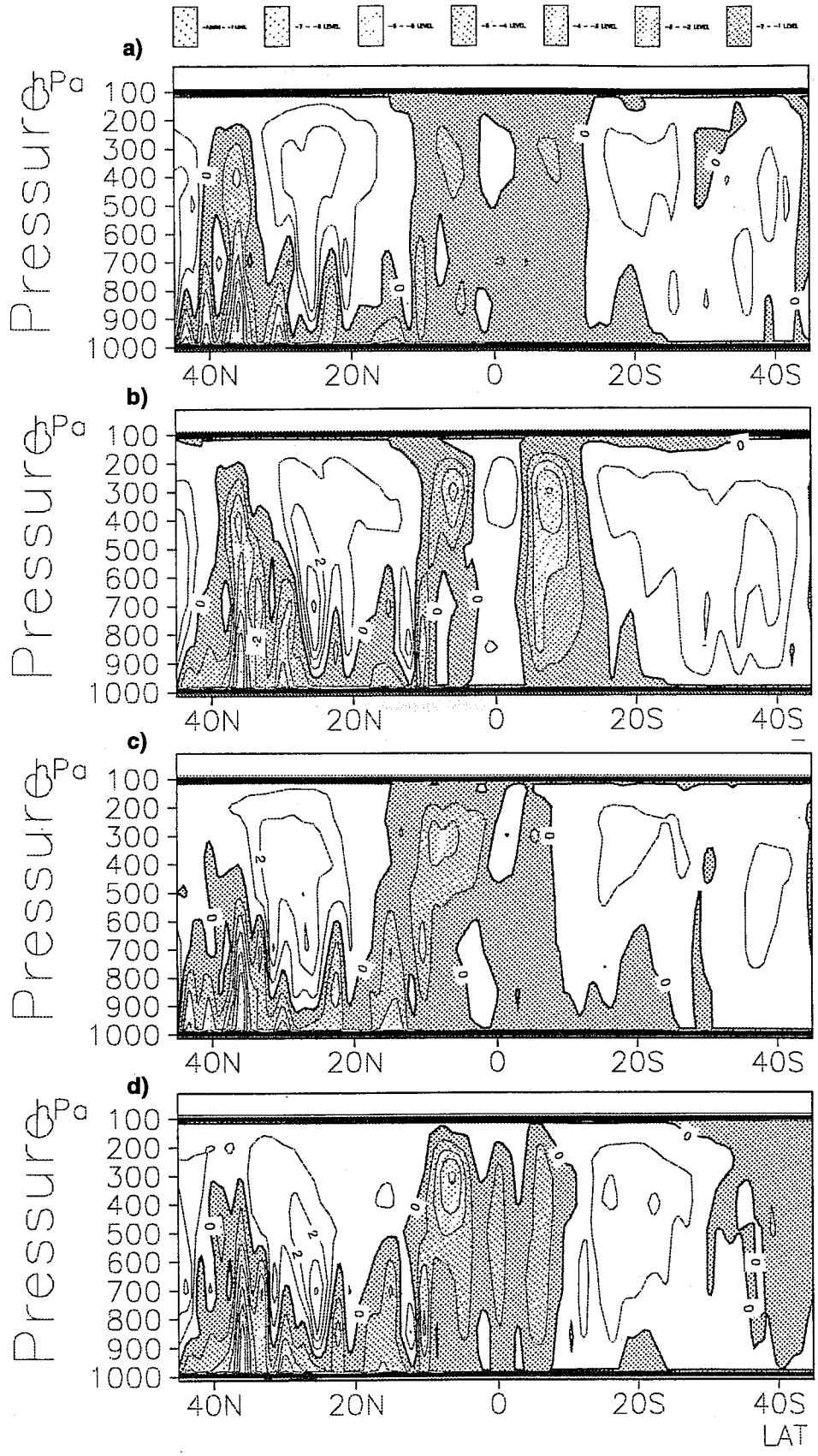

Fig 17 As in Fig 15 but for the vertical velocity.

as well as depth (Fig 15). There is a corresponding increase in the strength of the local branch of the Hadley cell indicated by the intensification of the cross-equatorial flow (low level southerlies and upper level northerlies, Fig 16) and increase in the rising motion north of the equator (Fig 17). The corresponding day-7 forecasts of these features shown in the right panels of the diagrams indicate that the model has produced excess upper level easterlies, relatively weak low level westerlies (Fig 15), a relatively stronger Hadley cell indicated by intense vertical motion (Fig 17), weak low level cross equatorial flow and upper level return flow (Fig 16) as compared to the analysis.

The pre-monsoon season of 1995 was characterised by three cyclonic storms which formed over the Bay of Bengal off the southeast coast of India and moved over land during 5-8 May, 9-13 May and 14-17 May. The direction of movement of the first storm was towards the northwest, while the last two moved in a north to northeast direction. These storms considerably influenced the circulation features over the region in this season and led to an unusual onset of the monsoon first over the northeast India on 5 June and later over the southwest coast of Kerala on 8 June.

The first storm formed over the Bay of Bengal near the Sri Lankan coast on 5 May and moved towards the northwest across the south Indian peninsula. Figure 18 shows that the model could predict the genesis of this storm about 36 hours in advance but its position was nearly 400 km east of the analysed position. The analysed and forecast tracks of this storm are illustrated in Fig 19. The diagrams indicate that there is a considerable difference between the observed (best track), analysed and predicted positions of the storm. It shows that initially the direction of movement was predicted properly towards northwest but, after reaching the Indian coast, the predicted directions were towards the north/northeast which were completely different from the observed direction of movement. Similar large differences between observed, analysed and forecast positions were also found for the other two storms which formed during 9-13 May and 14-17 May as shown in the lower panel of Fig 19. Table 3 shows the mean errors of these three storms computed with respect to the best track.

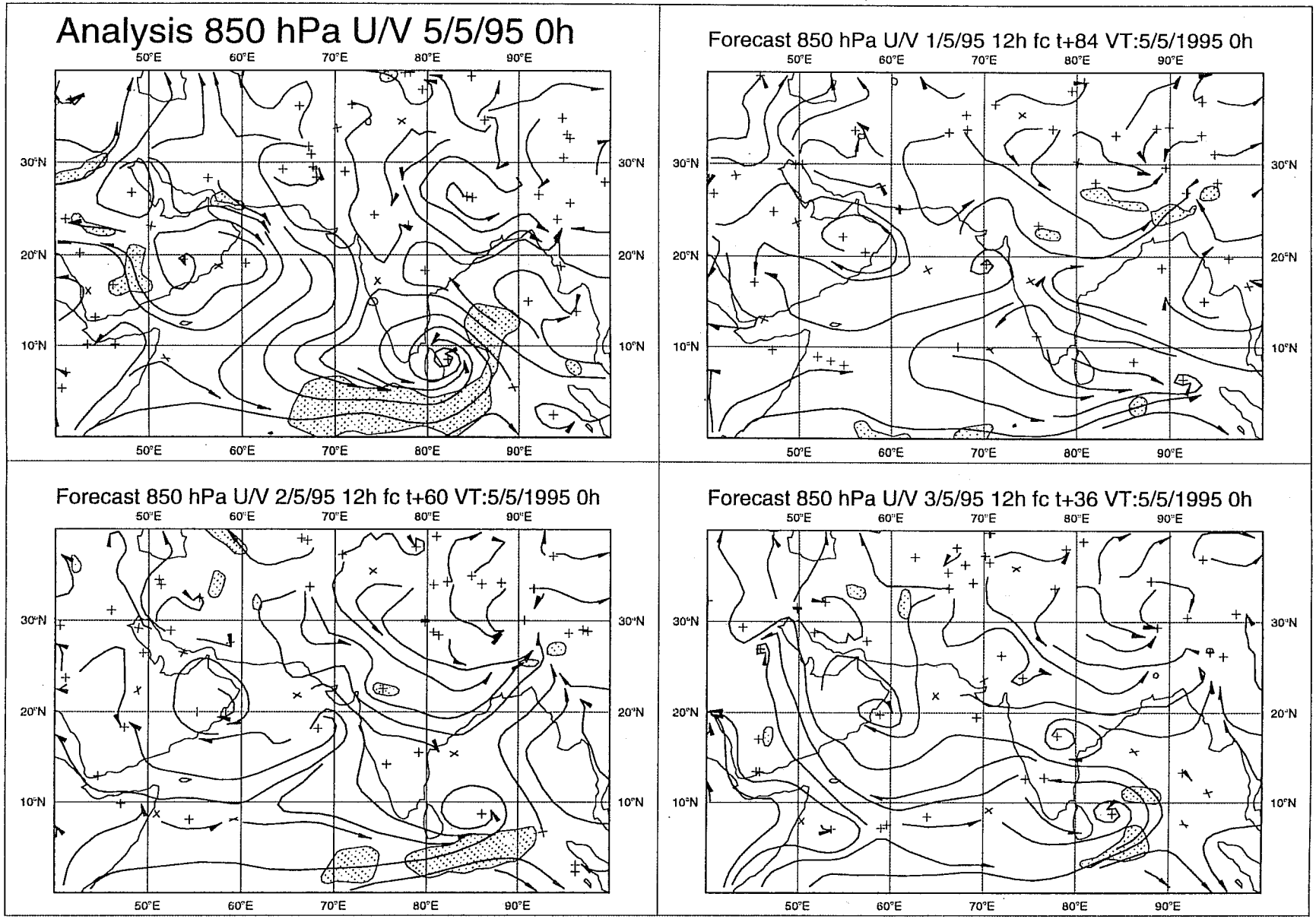

Fig 18 850 mb wind forecasts for 84, 60 and 36 hours and the corresponding verification analysis of 00 GMT, 5 May, 1995.

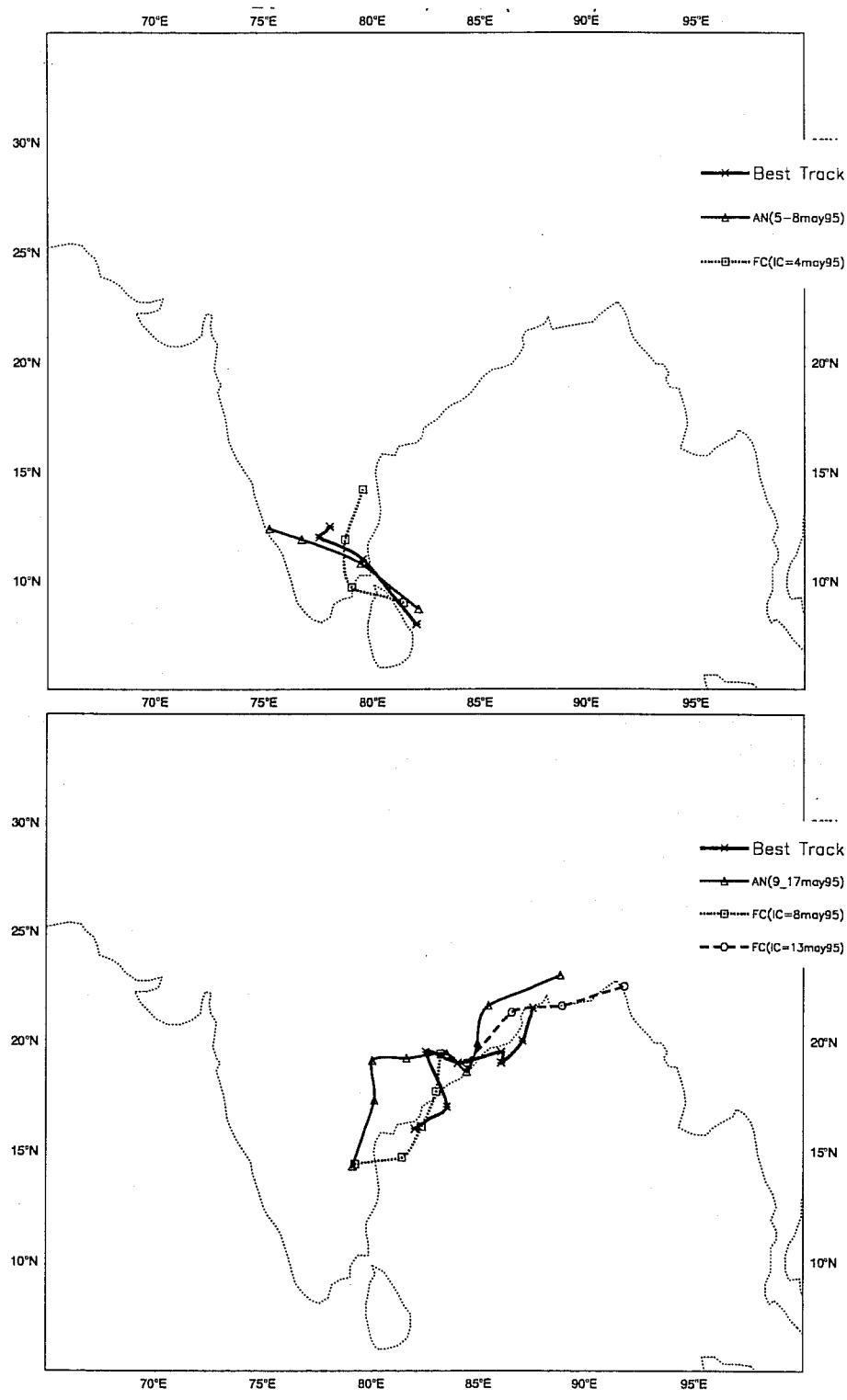

Fig 19 Observed, analysed and predicted tracks of the cyclonic storms over the period 5-8 May and 9-17 May, 1995.

Date	Analysis Errors (km)	Hours	Date of Initial Conditions 4 May	8 May	13 May	Mean
950505	79	12	129	349	168	215
950506	25	36	155	340	154	216
950507	88	60	131	379	145	218
950508	304	84	249	179		214
950509	364	108		294		294
950510	363					
950511	266					
950512	253					
950513	262					
950514	174					
950515	220					
950516	217					
Mean = 218						

Table 3: Cyclonic disturbances, 5-16 May, 1995

4.2 **The onset phase**

The onset of the monsoon is associated with a rapid intensification of the low level westerly jet over the Arabian sea, an upper tropospheric easterly jet over the south Indian peninsular and adjoining sea, an intensification of the Tibetan high at 150 mb, a shift of the westerly jet north of the Himalayas and commencement of rainfall over the southwest coast of India. In practice however, the onset of the monsoon is declared by the India Meteorological Department (IMD) only when there is rainfall of at least 1 mm on two coastal stations of Kerala continuously for two days, *Das* (1984). Studies by *Mohanty et al* (1984) indicated that there is a spectacular increase in the 850 mb kinetic energy over the Arabian sea just prior to the onset of the monsoon. This increase in kinetic energy is due to the coupling between intense convective heating, vertical motion and subsequent transfer of energy via divergent motion to the rotational part of the monsoon (*Krishnamurti et al*, 1995).

Fig 20 shows the time series of the kinetic energy at 850 mb level averaged over the area 0-20° N, 55-75° E. As mentioned earlier, the onset of the monsoon occurred over the Kerala coast on 8 June, while its arrival was declared over the north-eastern India on 5 June which was an unusual case in the last 20 years. Comparison of the time series of the kinetic energy between the years 1994, 1995 (Fig 20) and 1979 (Fig 2 of *Mohanty et al*, 1984) indicates that there were consistent increases of the kinetic energy at least for 2 consecutive days prior to the onset of the monsoon and its magnitude was about 25-30 m^2/sec^2 on the date of onset during those years, 1979 (11 June) and 1994 (28 May). In a recent study by *Ju and Slingo* (1995) a threshold value of 20 m^2/sec^2 was used to identify the dates of onset of the monsoon for ten years of climate integrations of the UGCM. Therefore, considering these facts, the model appears to have forecasted the onset of the monsoon on 6 June, 1995 based on the initial conditions of 1 and 2 June, 1995. Analysis of the Day-3 rainfall forecasts (Fig 21), however, indicate that the model was over-predicting the rainfall

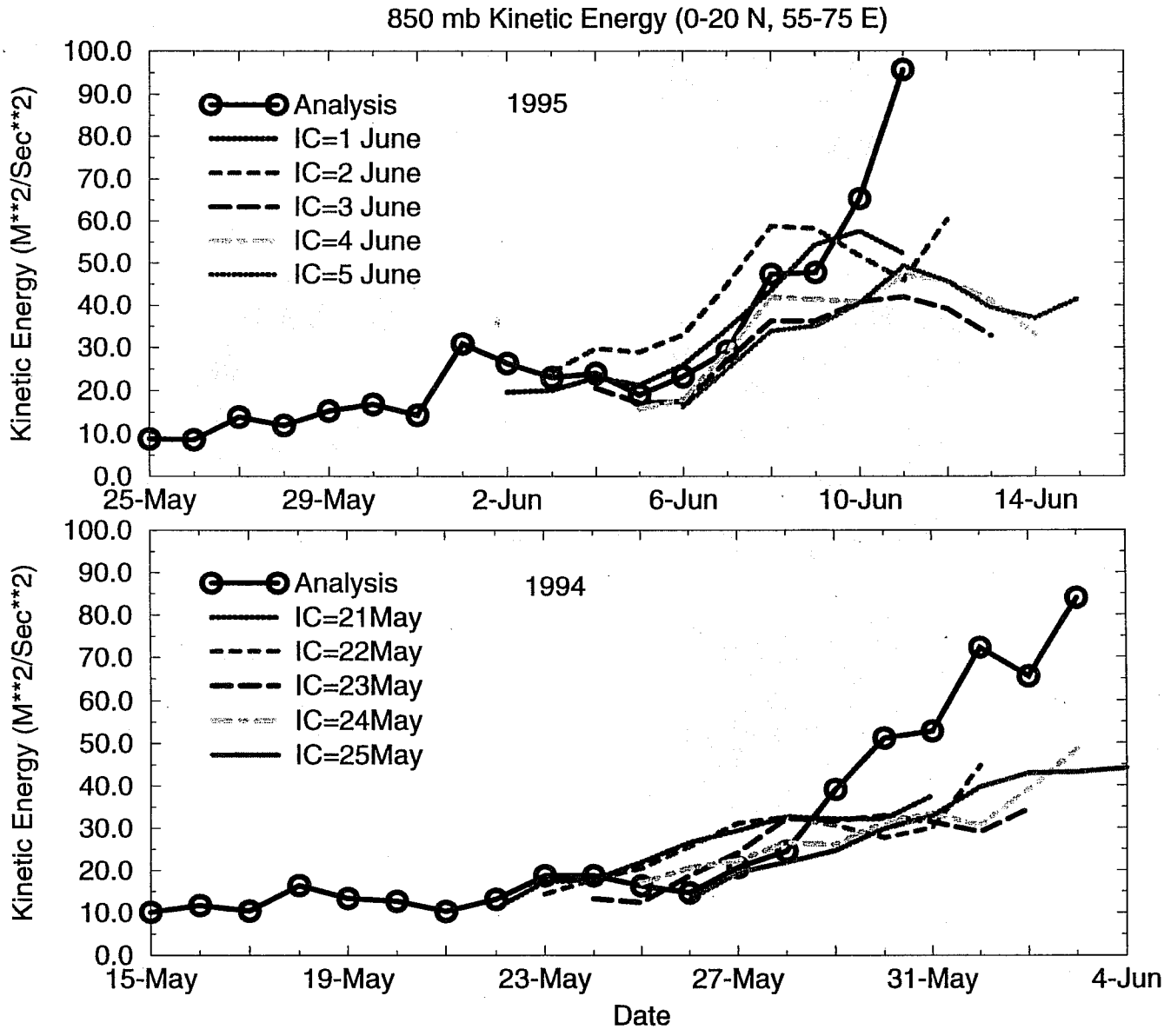

Fig 20 Time series of 10 day forecasts of 850 mb kinetic energy obtained from different initial conditions and the corresponding values obtained from the analysis.

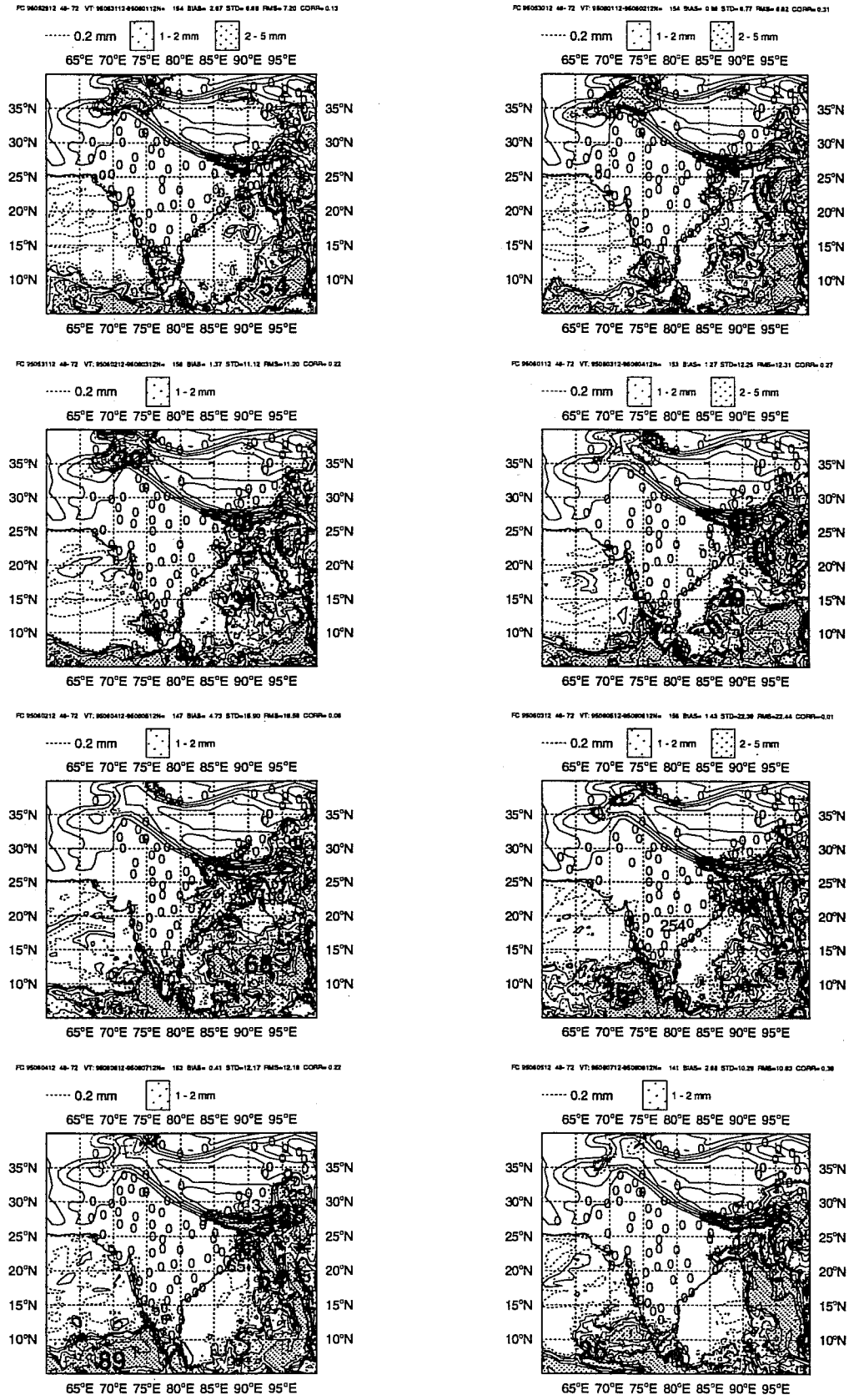

Fig 21 72 hour forecasts of rainfall valid for the period 1-8 June, 1995.

over the coast of Kerala continuously since June 4 and, as the commencement of rainfall is the primary factor considered for the declaration of the monsoon onset, a forecaster would have expected the date of onset on 4-5 June. Thus considering all these facts, the model appears to have predicted an early onset of the monsoon about two days before the actual date of occurrence.

4.3 The Active Phase

Fig 22 shows the 850 and 150 mb wind flow analysis and day-1, day-3 and day-7 forecasts averaged over the period 1-15 July. During this period the monsoon was very active and it had already covered the Indian subcontinent. As mentioned before, an active monsoon is characterised by a strong low level westerly jet (wind speed ~20 m/sec) over the Arabian sea and an upper level easterly jet at 150 mb. These features are reasonably well simulated by the model in its day-1 to day-7 forecasts although the model appears to have slightly underestimated the strength of the low level jet off the Somali coast. Moreover, the forecasts show smaller difluence of the 850 mb flow over the Indian peninsula as compared to the analysis.

Study of the positions of the monsoon trough (diagrams not shown here) indicated that the model had predicted a relatively stronger monsoon trough, but its position appeared to be satisfactory.

4.4 Monsoon lows/depression

The total rainfall during a monsoon season depends largely on the number of monsoon lows/depressions that form and move across the land. Accurate prediction of the areas of widespread heavy rainfall depends on how well the genesis and track of these systems are predicted. A number of such systems formed over the Indian region from June-September. Fig 23 shows the track of the two systems which formed and moved from 21-26 July and 28 August to 3 September. The prediction of the genesis of these systems was indicated only about 12-24 hours in advance by the model. There were also large differences between the analysed and forecast tracks of these storms as in the case of 1994 and those of May, 1995. However, the direction of the movement was reasonably good in the forecasts. The errors between the observed and predicted tracks may be due to the fact that no Indian radiosonde observations are used in the analysis. Better use of INSAT and TEMP data may improve the simulations of these systems in future.

4.5 Rainfall, total cloudiness and 2 metre temperature

In this section we shall discuss the average performance of the model in forecasting the total precipitation, cloudiness and 2 metre temperature during May to August, 1995. Fig 24 illustrates the time series of bias, RMSE and correlation coefficients of 36-60 hour forecasts of total precipitation averaged for the 15 day periods from 1-15 May, 16-31 May, 1-15 June, 16-30 June, 1-15 July, 16-31 July, 1-15 August and 16-31 August over Europe (25-60° N, 18° W - 70° E) and the Indian region (5-40°N, 60-100° E). The diagram indicates that the bias as well as RMSE of rainfall increases from pre-onset to the onset phase, remains high during the active monsoon

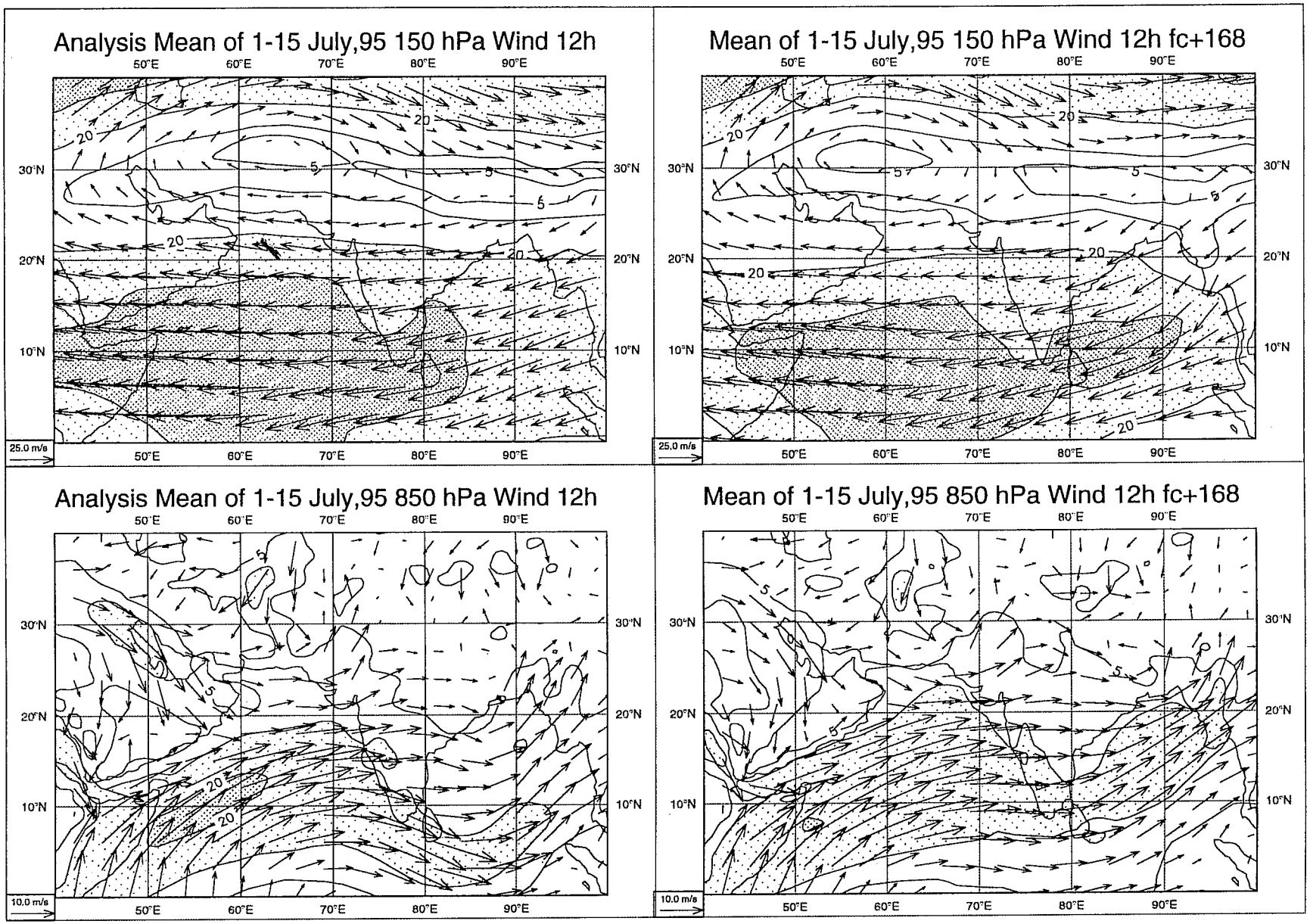

Fig 22 850 and 150 mb wind analysis and the corresponding Day-7 forecasts, averaged over the period 1-15 July, 1995.

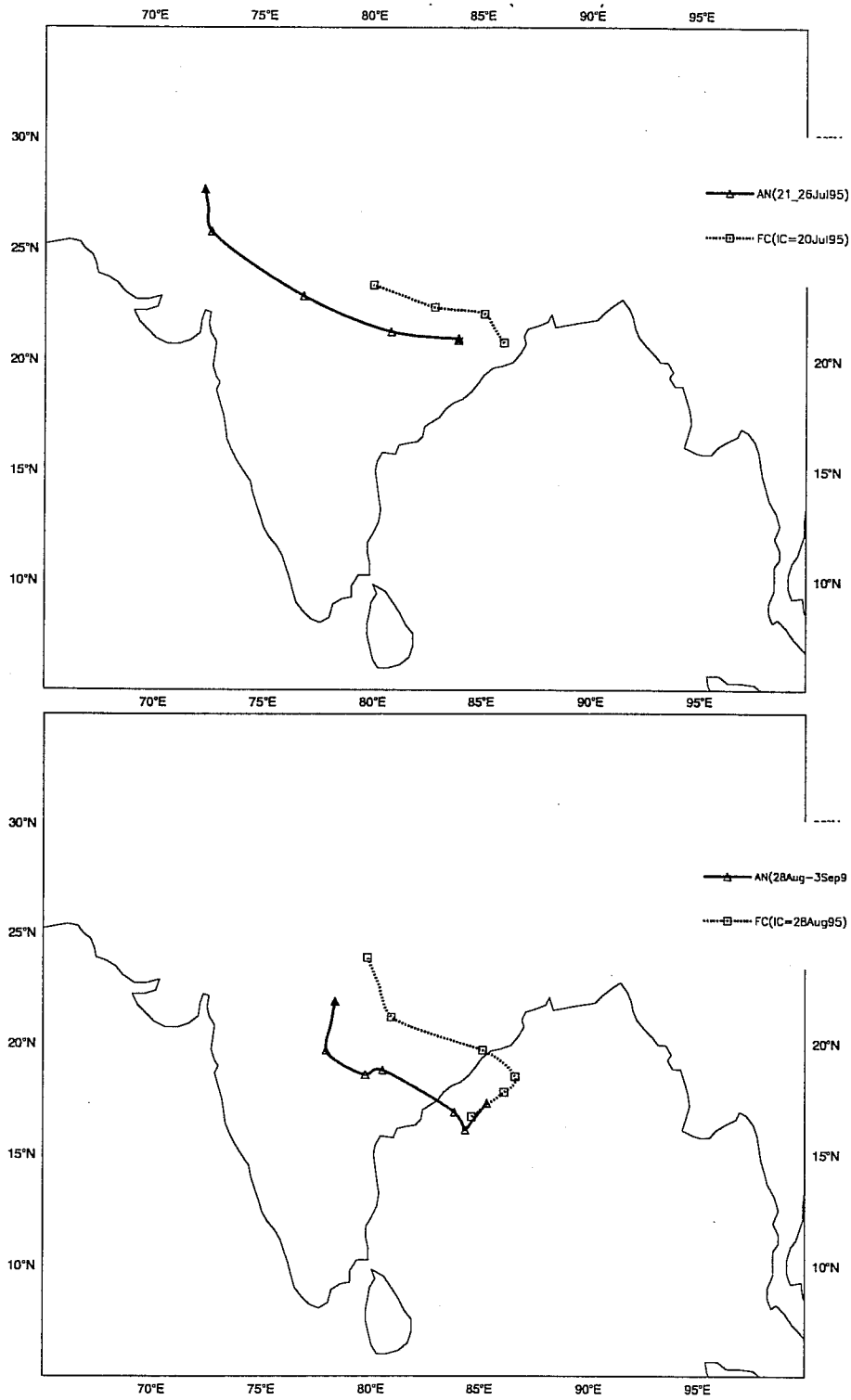

Fig 23 Analysed and predicted tracks of the Monsoon lows for the periods 21-26 July and 28 August - 3 September, 1995.

and decreases subsequently. The correlation is lowest during the peak monsoon phase. Comparison of the forecasts shows much better performance over the Europe than over the Indian region during these months. The geographical distribution of the errors (Fig 25) shows that, as the monsoon season progresses, the model overestimates rainfall over the mountains and relatively underestimates over the plains. Table 4 presents the Threat Scores of predicted rainfall starting from 1 May to 31 August.

	Rainfall range (mm/day)				
	0-0.1	0.1-2	2-5	5-20	20-999.0
1-15 May	0.65	0.06	0.03	0.09	0.38
16-31 May	0.67	0.04	0.06	0.07	0.07
1-15 June	0.65	0.02	0.03	0.08	0.28
16-30 June	0.38	0.1	0.07	0.11	0.16
1-15 July	0.35	0.11	0.01	0.13	0.26
16-31 July	0.16	0.12	0.08	0.15	0.2
1-15 Aug	0.18	0.13	0.05	0.13	0.09
16-31 Aug	0.18	0.1	0.05	0.13	0.15

Table 4: Threat score

The scores have been computed based on the rain gauge stations over India (Blocks 42 and 43) and the rainfall forecasts are for the range 36-60 hours. A threat score 1 indicates the best forecast. The table shows that the best predictability of the model is for the rainfall range 0 to 0.1 mm (no rainfall or drizzle) during the premonsoon season. The scores deteriorates with the progress of the monsoon. Table 5 presents a contingency table of the absolute frequency of the rainfall forecasts from 1 May to 31 August.

	OBSERVED mm/24 h					
class	0-0.1	0.1-2	2-5	5-20	20-999.0	
999.00						999.00
F	142	85	58	154	216	
O 20.00						20.00
R	683	311	143	262	231	
E 5.00						5.00
C	508	153	66	123	76	
A 2.00						2.00
S	1124	218	91	121	79	
T 0.10						0.10
	2265	126	59	82	39	
0						0
class	0	0.10	2.00	5.00	20.00	999.00

Table 5: Contingency table of absolute frequency

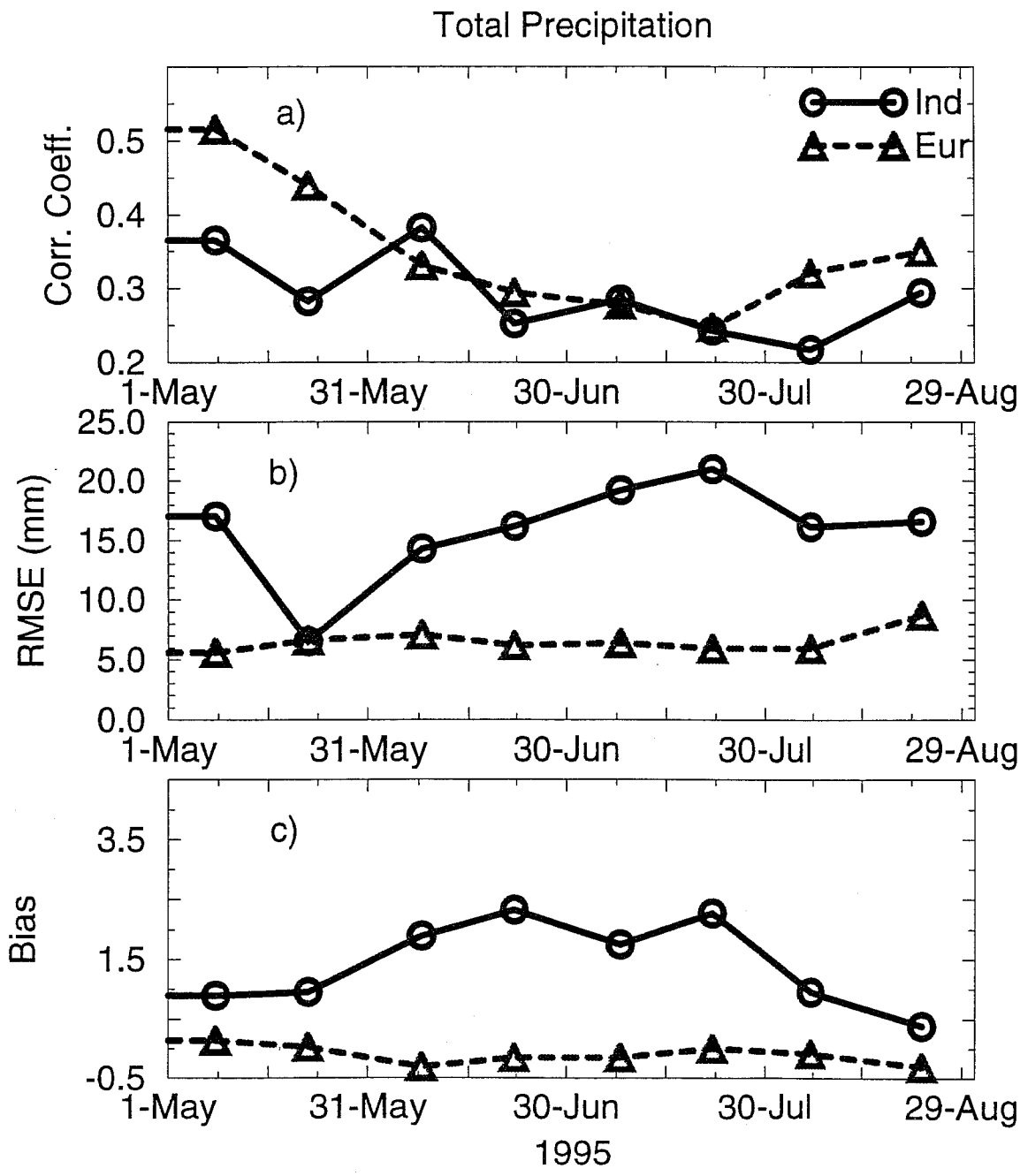

Fig 24 Mean of 60 hour forecast Bias, RMSE and Correlation Coefficients of the total precipitation obtained over the Indian region and Europe for the periods 1-15 May, 16-31 May, 1-15 June, 16-30 June, 1-15 July, 16-31 July, 1-15 August, 16-31 August, 1995.

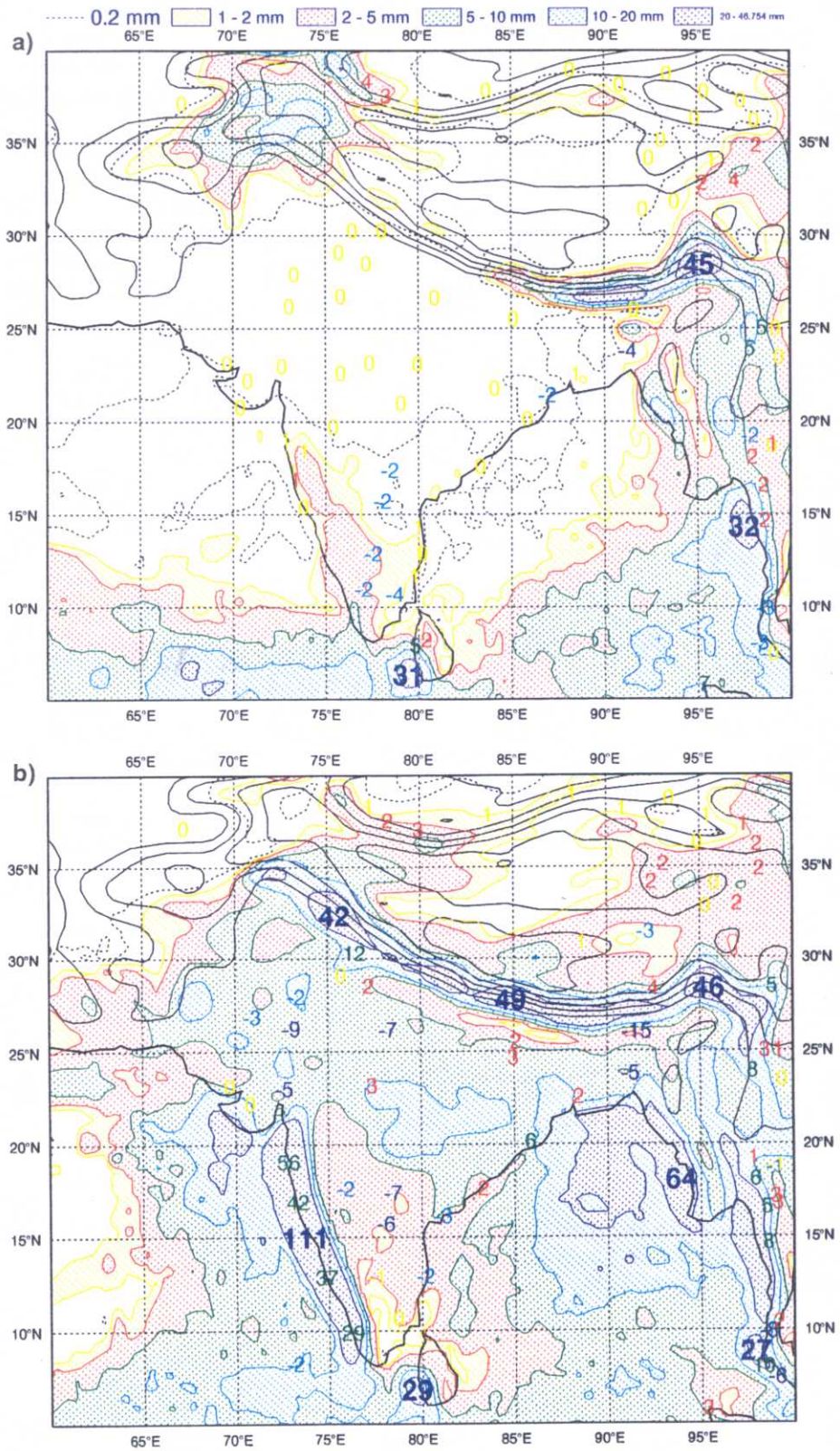

Fig 25 As in Fig 2 but for 60 hour forecast over the periods 16-31 May and 16-31 July, 1995.

It is seen from the above table that the highest frequency of correct rainfall forecasts is for the range 0 to 0.1 mm/day. In other words, the model is good for predicting only a 'YES/NO' rainfall over the monsoon regime. For observed rainfall values greater than 20 mm/day the model has a tendency to predict rainfall between 5-20 mm/day.

The time series of the 60 hour forecasts of total cloudiness (Fig 26) shows that the model underestimated the cloudiness during the active monsoon periods (15-30 June and 16-31 July). Comparison of values over Europe (at a different local time, 00 GMT) shows mixed results. The geographical distribution of cloudiness (Fig 27, 28) shows that, during the pre-onset phase (16-31 May), the model relatively underestimated the cloudiness over the southern peninsular, while during the active phase (16-31 July) it underestimated the cloudiness over central and north India which are the zones of heavy cloudiness during this season.

Study of the forecasts of the 2 metre temperature (Fig 29) indicates that there is a very strong cold bias during the pre-onset phase in the clear sky conditions which is also indicated in diagram 33. Values as cold as -9 to -10° C (absolute errors) are seen over north India during morning hours in this period. This is apparently related to the deficiency of the model in transporting heat flux towards lower soil layers. The surface loses heat too rapidly by radiative cooling in order to maintain the equilibrium in clear sky conditions. The errors are considerably reduced in the active monsoon phase when there are more clouds over the region (Fig 28). The performance over Europe is again better (Fig 29) during the entire period.

5. SENSITIVITY EXPERIMENTS

As mentioned earlier, the current operational model CY13R4 has a tendency to overestimate rainfall over the Western Ghat (see Fig 2b and 25b) and often fails to predict widespread convective rainfall over land areas east of the Ghat mountains (Fig 30). In order to understand the reason for failure of the model in forecasting the widespread rainfall, a few sensitivity experiments have been carried out with the new Subgrid Scale Orography (SSO) and prescribed initial soil moisture over India which are described as follows.

5.1 **Subgrid Scale Orography**

In order to understand whether the new parametrization of SSO produces an excessive rainshadow effect, experiments were carried out by switching off the new SSO scheme and the model was run for 5 days using three initial conditions of 12, 13 and 14 July. However, for brevity here we shall mainly describe the results of the last experiment run with the initial condition of 14 July. The experiments are summarised in the following table.

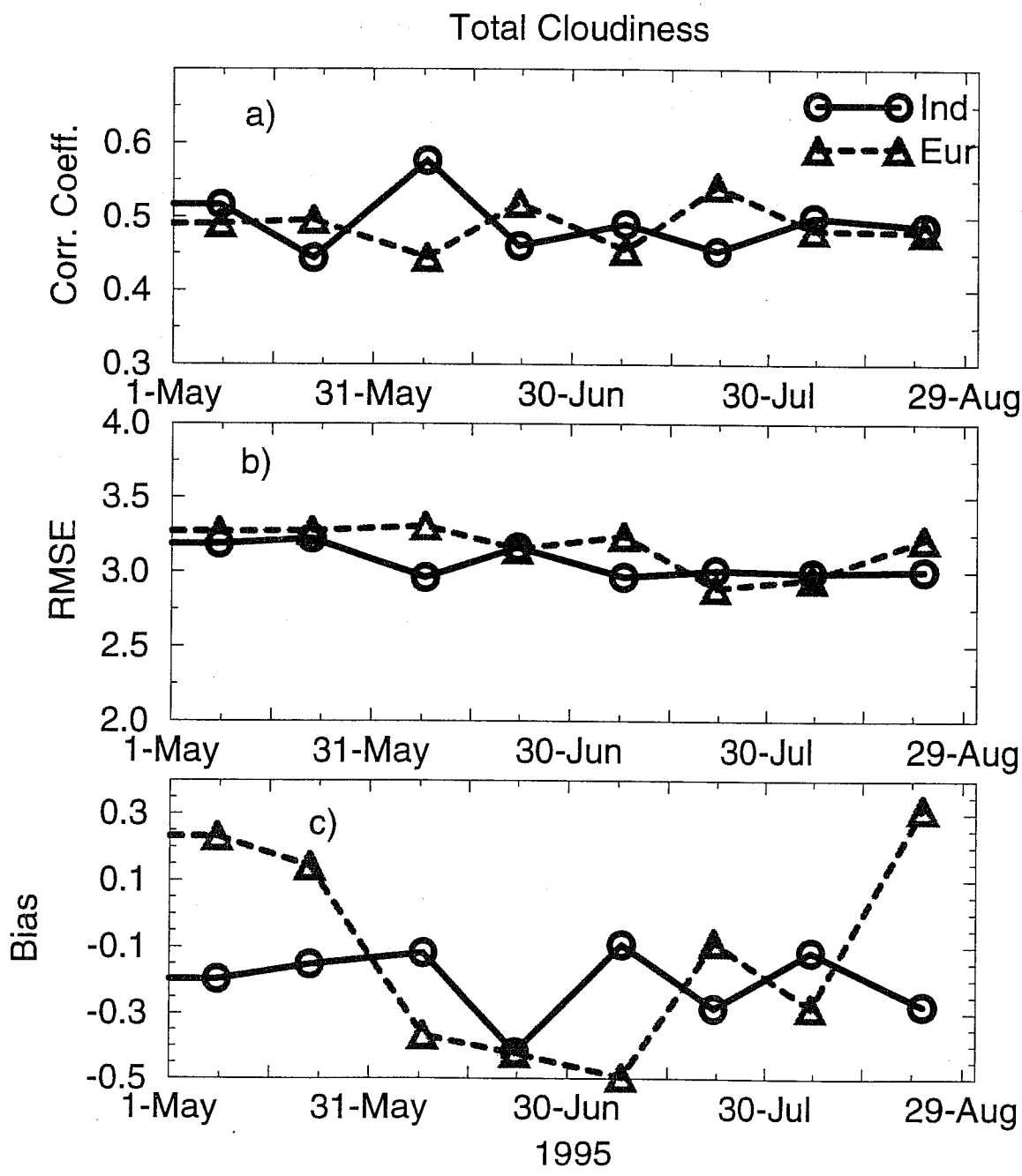

Fig 26 As in Fig 24 but for the Total Cloudiness.

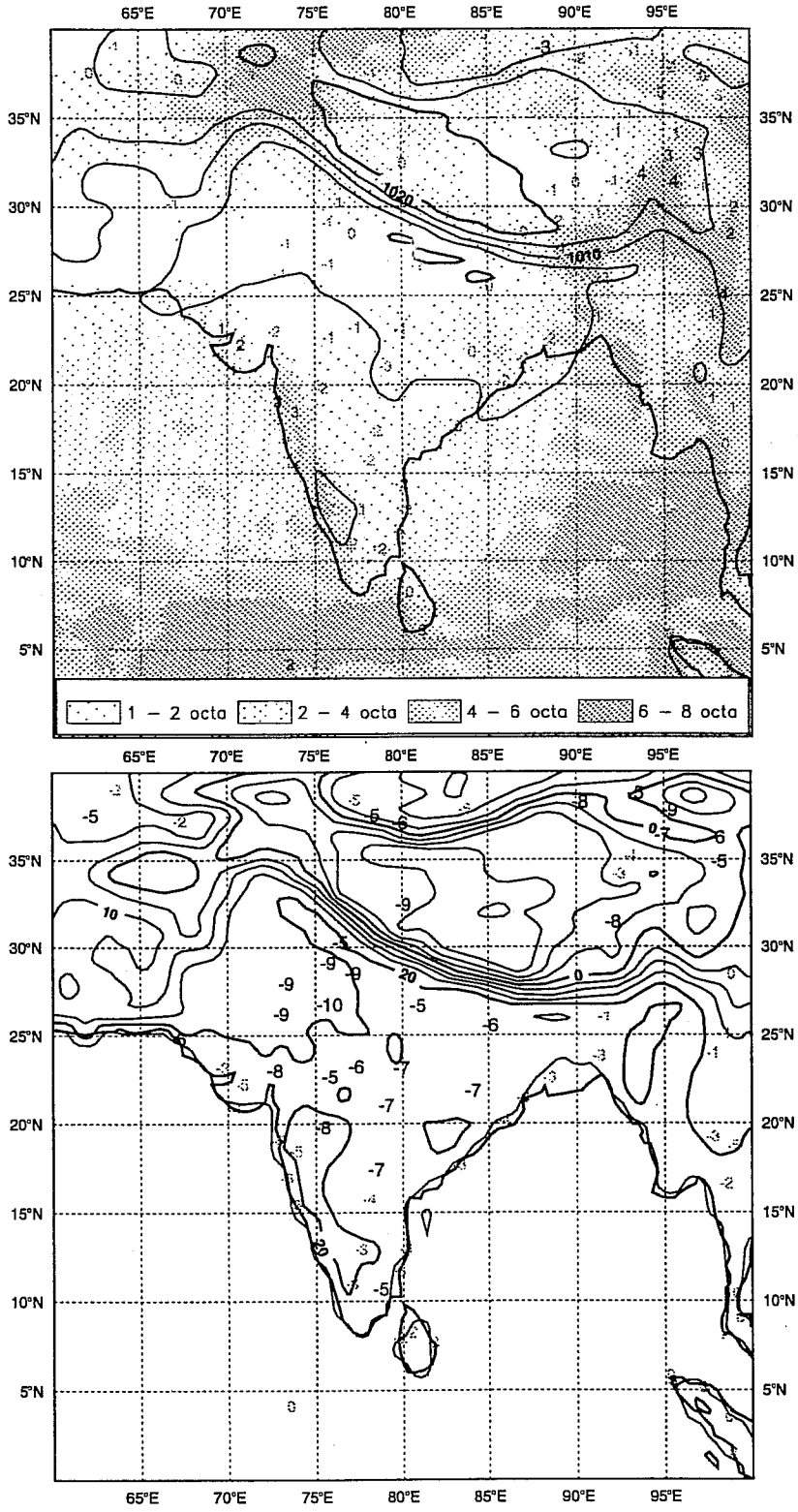

Fig 27 As in Fig 2 but for 60 hour forecasts of total cloudiness and 2 metre temperature for the period 16-31 May, 1995.

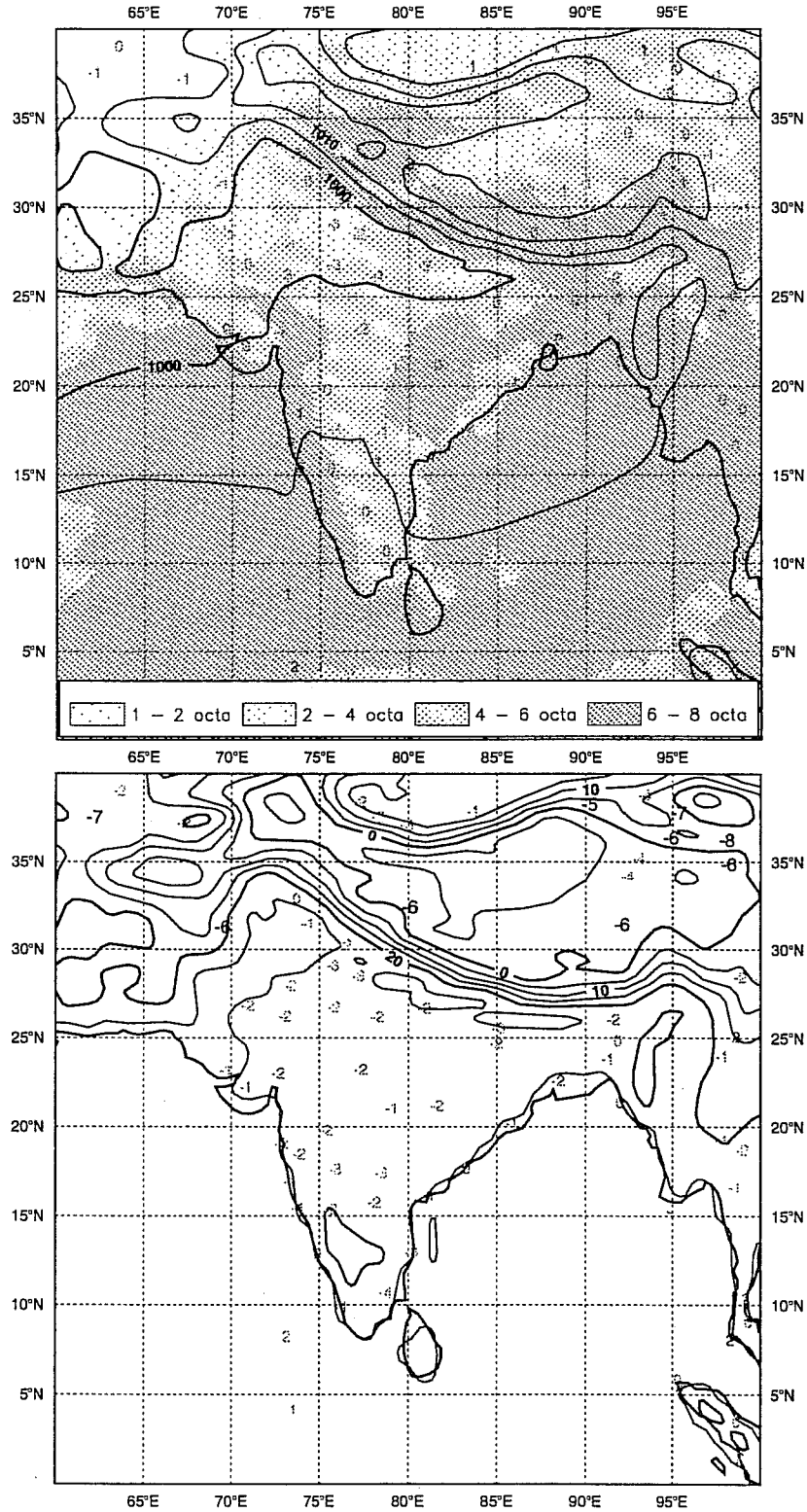

Fig 28 As in Fig 2 but for 60 hour forecasts of total cloudiness and 2 metre temperature for the period 16-31 July, 1995.

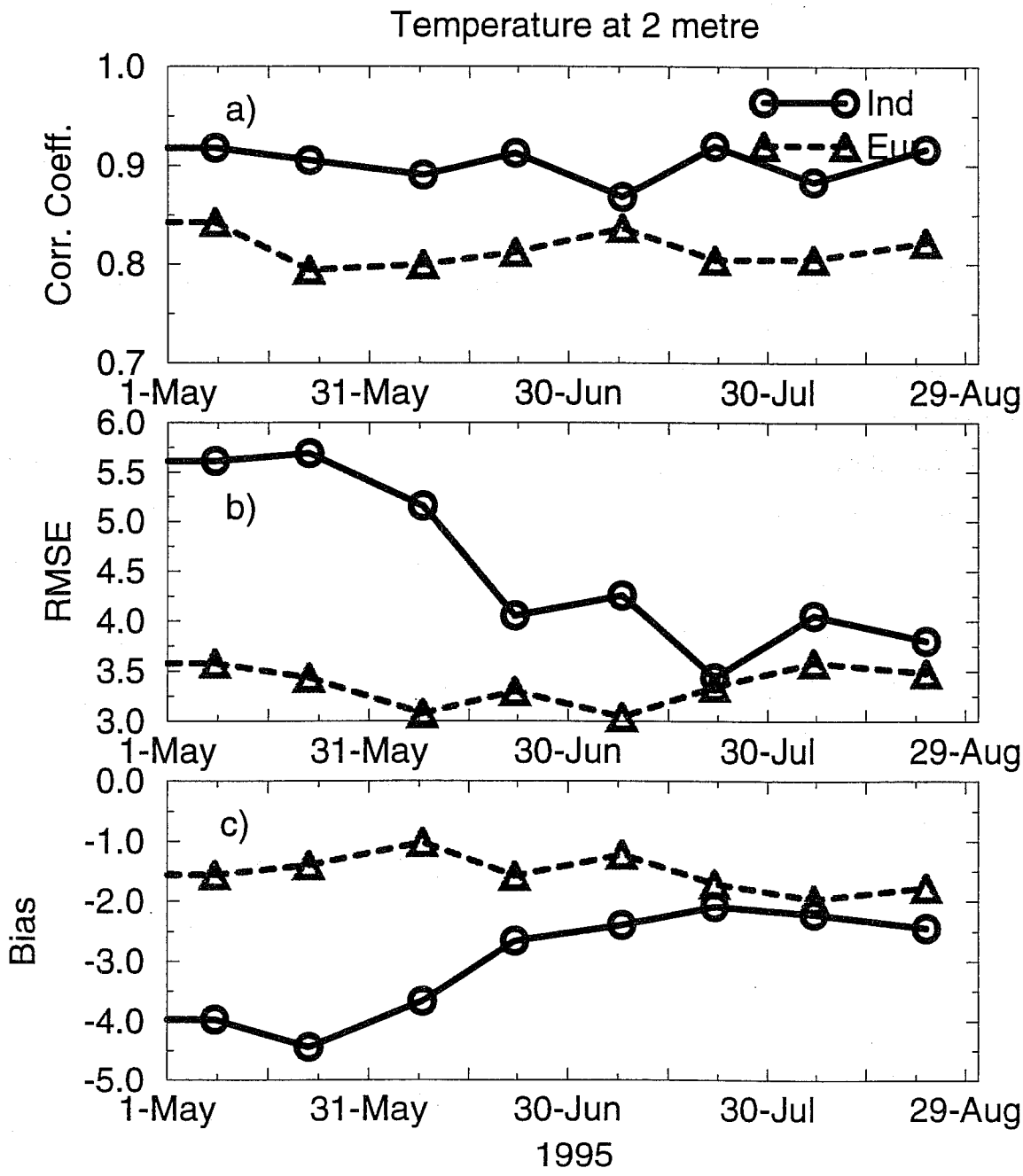

Fig 29 As in Fig 24 but for the 2 metre temperature.

Name of the Experiment	Description
OPER	Control runs with operational model
ZIVO	No subgrid scale orography (12 July)
ZILO	No subgrid scale orography (13 July)
ZILP	No subgrid scale orography (14 July)

Table: 6 Summary of experiments on SSO

Fig 31 shows the 60 hour rainfall forecasts obtained from experiments ZIV0 and ZILP. As seen from the diagrams, there is very little difference between the rainfall forecasts obtained from the control runs (Fig 30) and the experiments (Fig 31). On the other hand, the operational model produces more realistic areas of convergence on either side of the mountain as seen from the rising motion (Fig 32) by allowing a part of the flow to go around the flank of the hills and producing less blocking effect on the windward side. As a consequence, more cloudiness is also simulated downstream away from the mountains by OPER than compared to ZILP (figure not shown here). Similar results were also obtained from the experiments ZIV0 and ZILO.

In order to further investigate the cause of failure of forecasting the widespread rainfall, Fig 33 shows the observed and predicted tephigrams of Madras, 13° N, 80° E (Index=43279). The diagrams show strong unstable profiles of observed temperature and moisture. The first guess profiles (light dotted) show that the model is warmer and dryer compared to the observations. Consequently, the predicted tephigram (Fig 33b) shows weakly unstable to neutral profiles as well as a dryer boundary layer. Similar profiles were also observed for other surrounding stations. The drying effect was further confirmed from the difference between the forecast and verifying analysis of the specific humidity. The problem was therefore further investigated by conducting four experiments with prescribed soil moisture as described in the next section.

5.2 **Soil moisture**

The dry lower layers of the atmosphere as discussed in the previous section could be related to too small values of soil moisture over the Indian subcontinent. Four experiments were therefore conducted by flooding and drying the soil over the Indian region (5-35° N, 70-95° E) with the initial conditions of 12 and 14 July, 1995. The experiments are summarised in Table 7. The model was run for 5 days from each of the initial conditions.

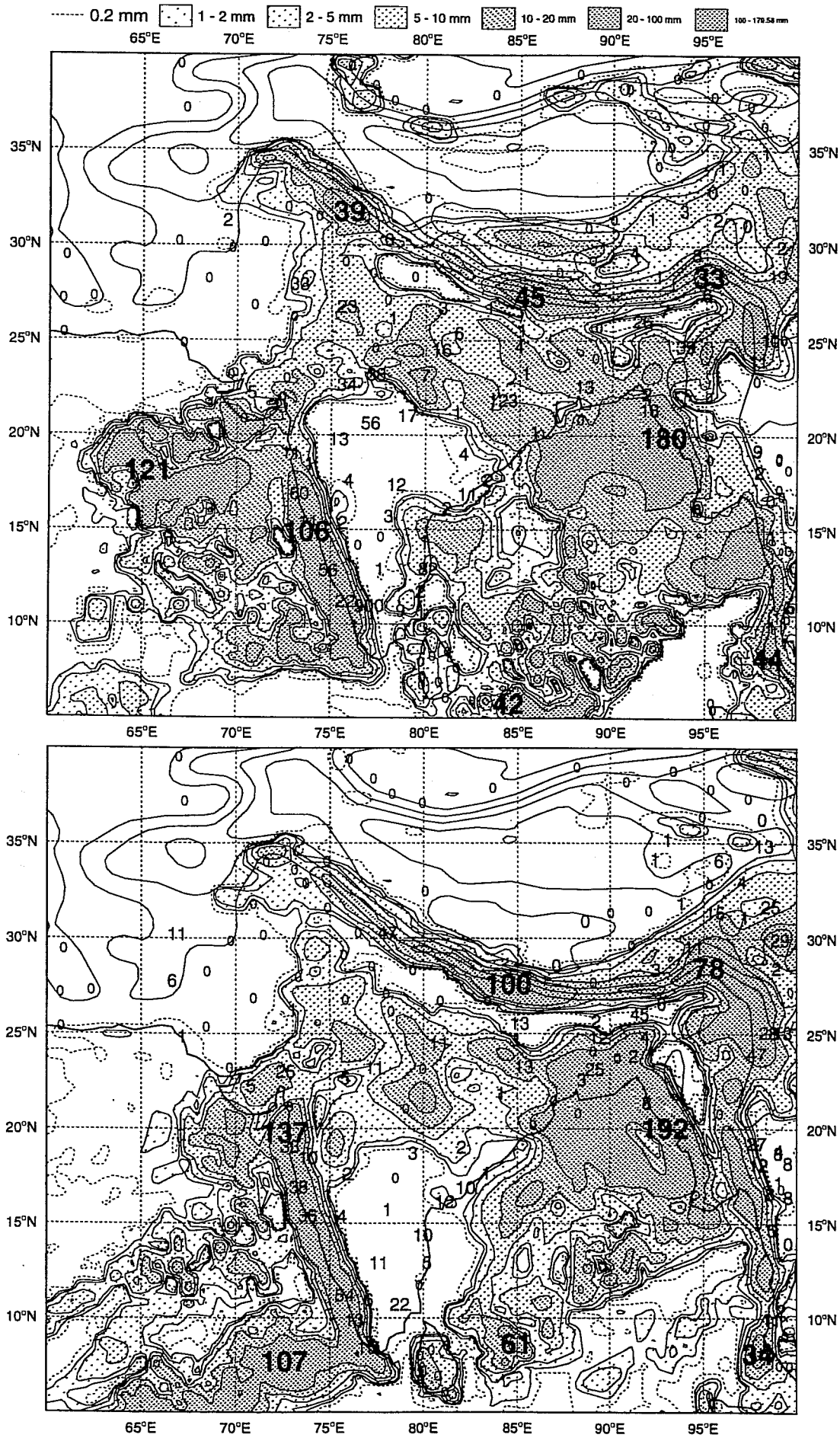

Fig 30 60 hour rainfall forecasts based on the initial condition of 12 and 14 July, 1995 obtained from the operational model.

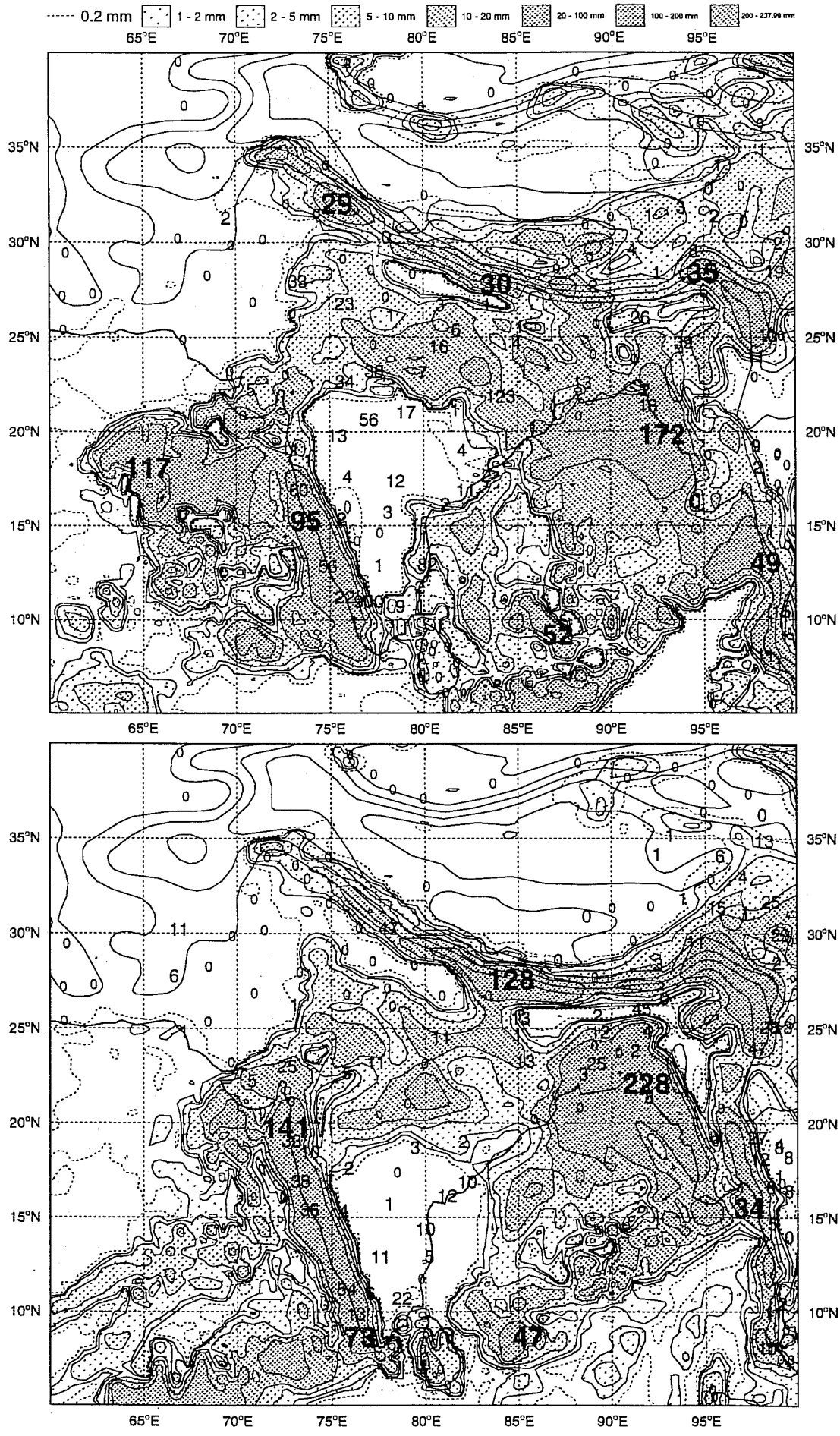

Fig 31 As in Fig 30 but for experiments (a) ZIV0 and (b) ZILP.

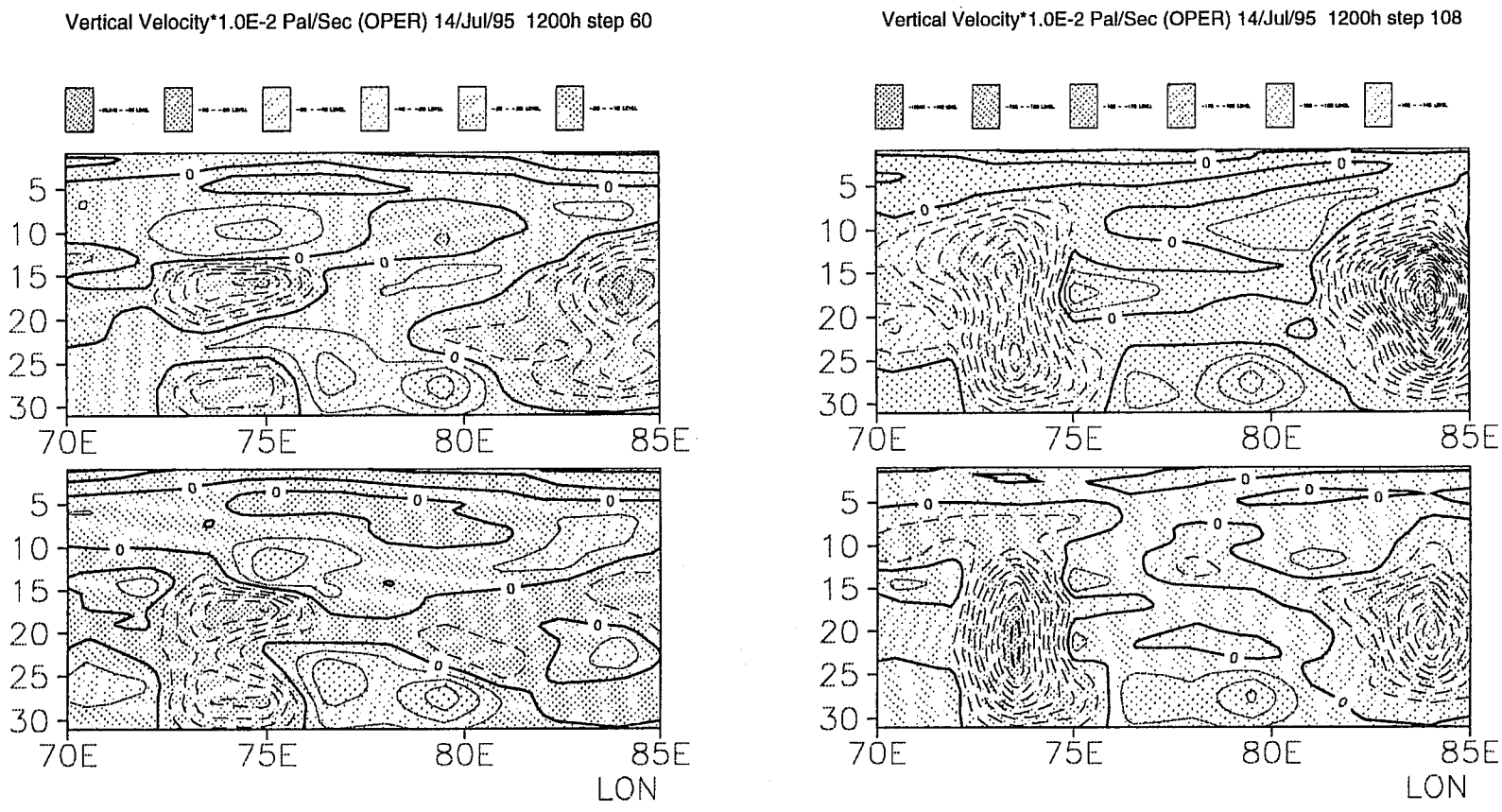

Fig 32 Vertical cross sections of the vertical velocity obtained for 60 and 108 hour forecast from the initial condition of 14 July, 1995 obtained from OPER and ZILP.

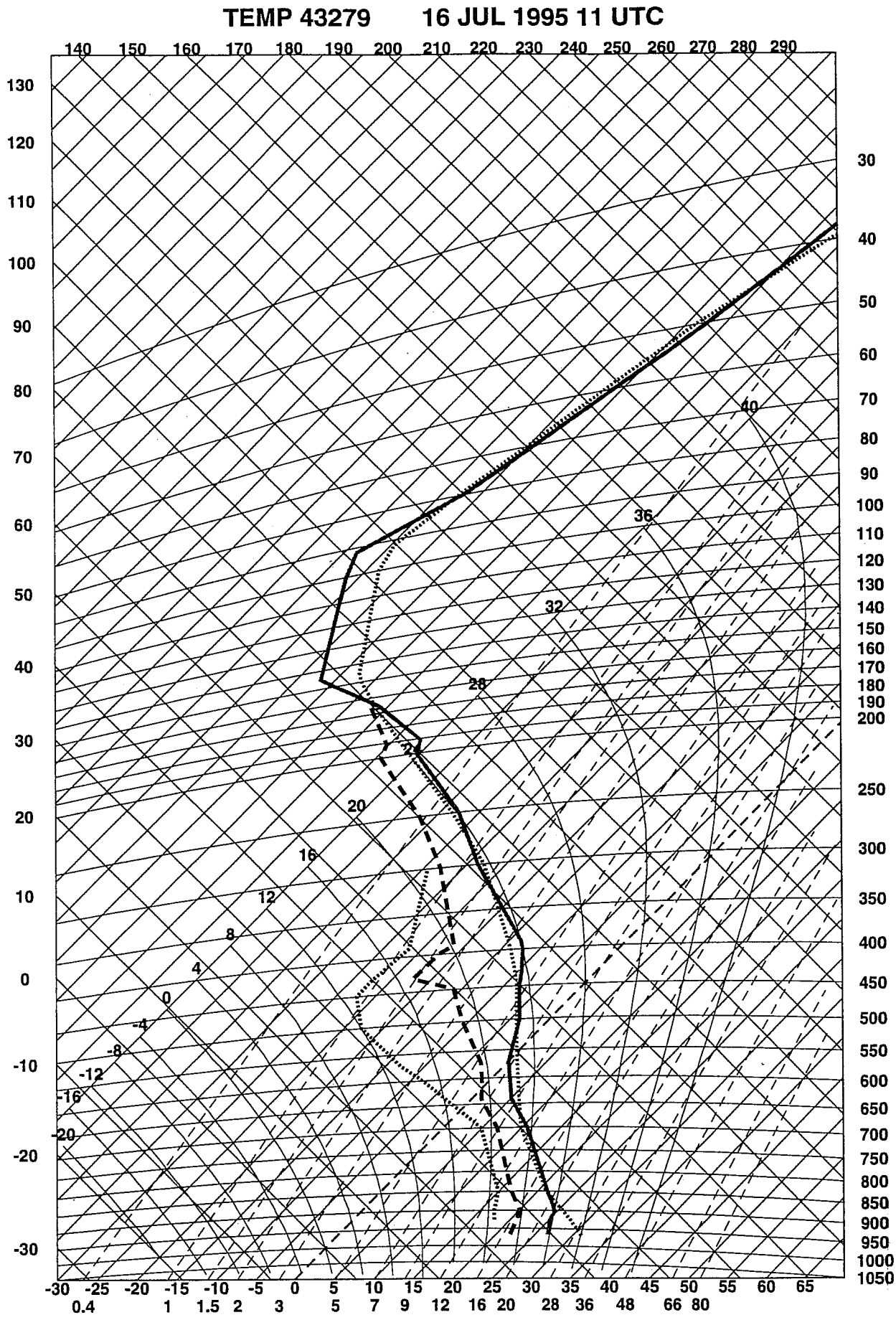

Fig 33 | a) Observed Tephigram of Madras.

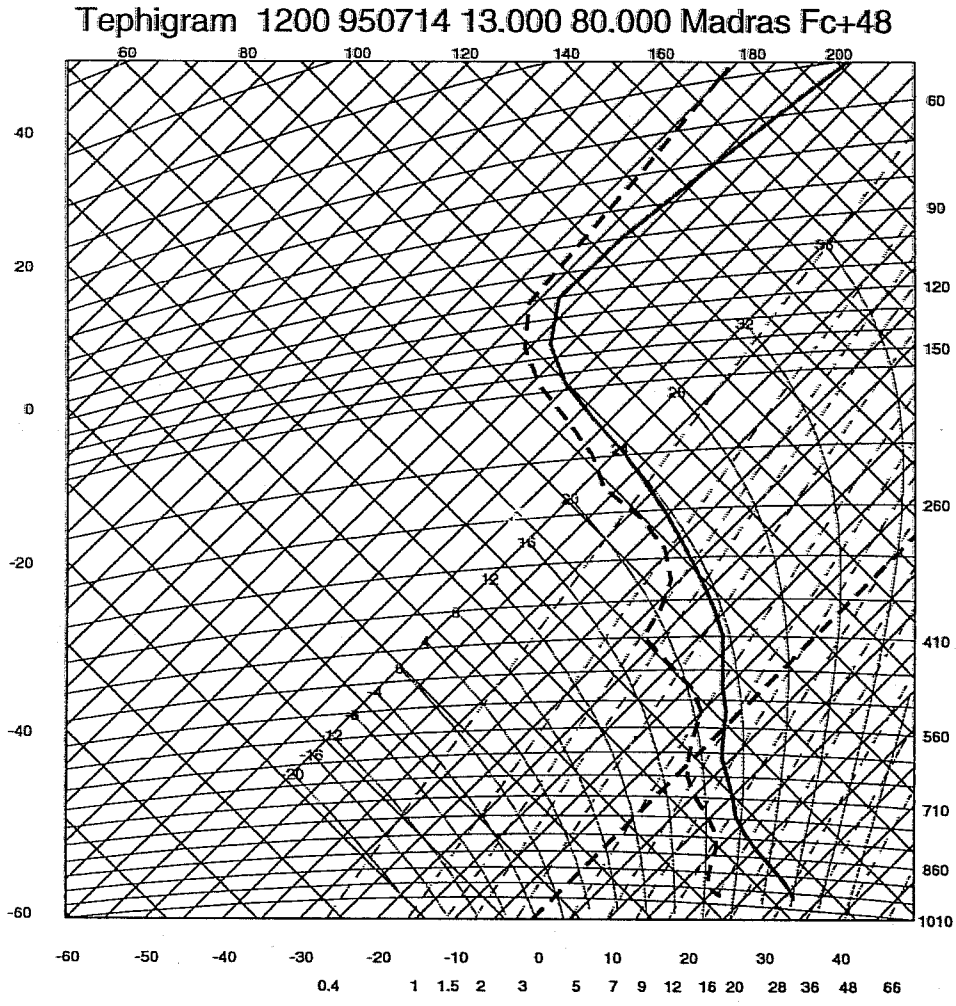

Fig 33 b) 48 hour forecast Tephigram of Madras

Name of the Experiment	Description
OPER	Control runs with operational model
ZIRC	Flood soil (Initial condition = 14 July)
ZIT5	Flood soil (Initial condition = 12 July)
ZIT6	Dry soil (Initial condition = 14 July)
ZIT7	Dry soil (Initial condition = 12 July)

Table: 7 Summary of experiments on soil moisture

Figures 34, 35 illustrate the 60 hour rainfall forecasts obtained from experiments ZIT5, ZIT7, ZIRC and ZIT6. As seen from the diagrams, there are very little differences between the rainfall forecasts obtained from the operational model (Fig 30) and the four experiments. The model appears to be very robust to the changes in the soil moisture over the Indian region as far as medium-range forecasts of rainfall are concerned. Thus the problem does not appear to be simple. However, these experiments provide several insights into the physical mechanisms involved in the process. The wet experiment ZIRC leads to increased evaporation from the surface (Fig 36) leading to cooling at the ground. This results in a decrease in the sensible heat but an increase in the latent heat flux at the surface (Fig 37). The moistening and cooling caused by evaporation at the surface were reflected in the tephigrams (not shown here) which showed a relatively moist and cold surface layer at Madras and Karaikal in the 48 hour forecast. The resulting thermodynamic profiles show very weak conditionally unstable layer. At this stage the large scale dynamics also plays its role. The cooling at the surface may lead to slackening of the pressure gradient and rise in the sea level pressure leading to increased subsidence and decrease in the rising motion (diagrams not shown here). This prevents the enhancement of convection and associated condensation (Fig 38) and results in a continued dry troposphere (Fig 39). The overall processes lead to decreased cloudiness and continued underestimation of rainfall over the area. However, the fact that the dry experiments ZIT6 and ZIT7 also do not produce any significant change in the rainfall forecasts indicates the existence of more complicated mechanisms that need to be understood. It is possible that there is a deficiency in the moisture transport mechanism of the model and the closure scheme of the convective parametrization is not realistic. At this stage the solution of the problem remains incomplete. Further investigations are required on the closure schemes and formulation of clouds in the model.

6. CONCLUSIONS

The prognostic cloud scheme and the new parametrization of subgrid scale orography are the two major changes in the physical processes of the current operational model. Comparison of the combined influence of these two changes against the old version of the model indicates better forecasts of the cloudiness and 2 metre temperature by correcting the negative cloud bias and warm surface bias of the old model. With regard to rainfall, while the old version underestimated the total precipitation over the western Ghat mountains, the new version overestimates the rainfall over there. The current model produces larger positive bias and higher RMSE of

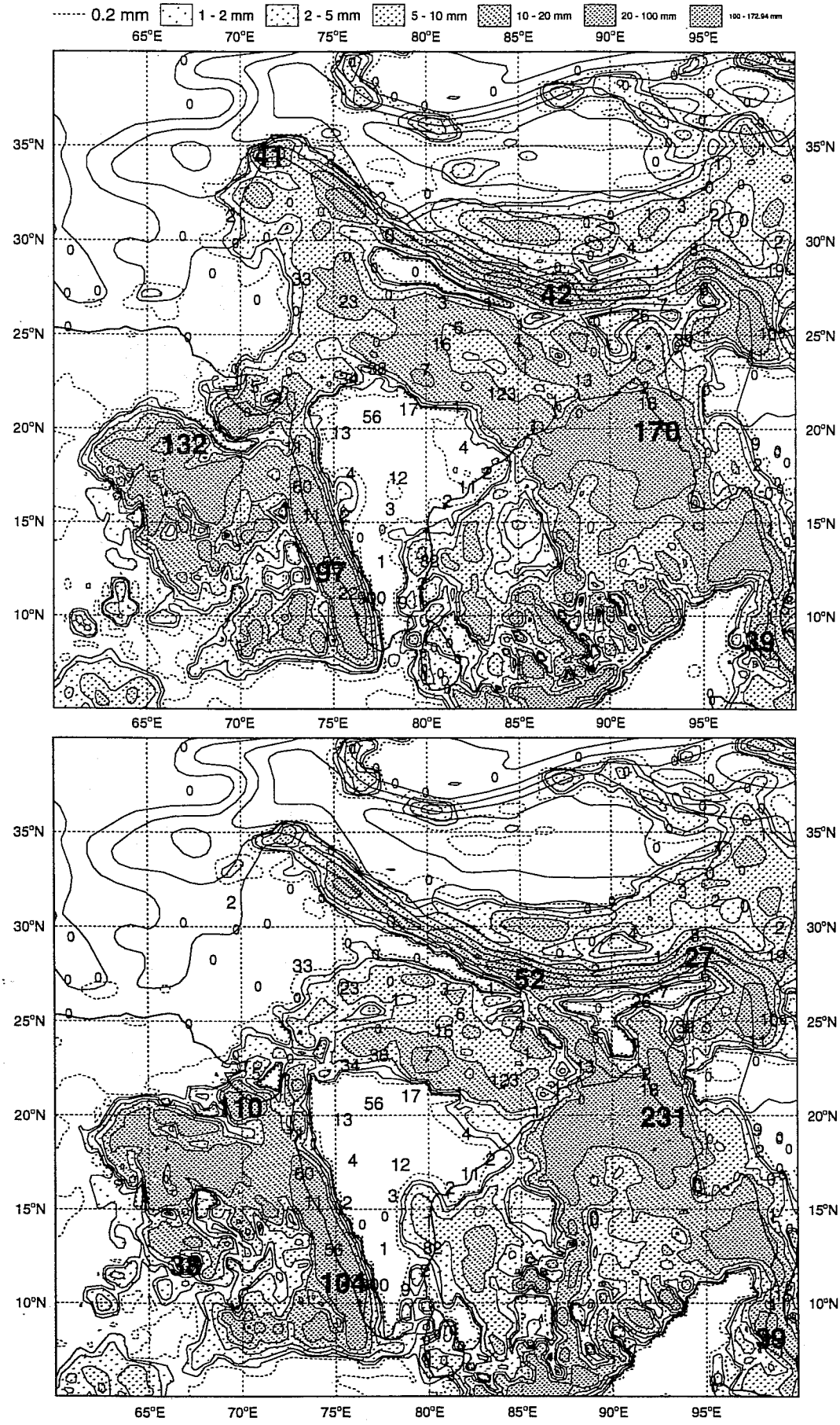

Fig 34 As in Fig 30 but for experiments ZIT5 and ZIT7.

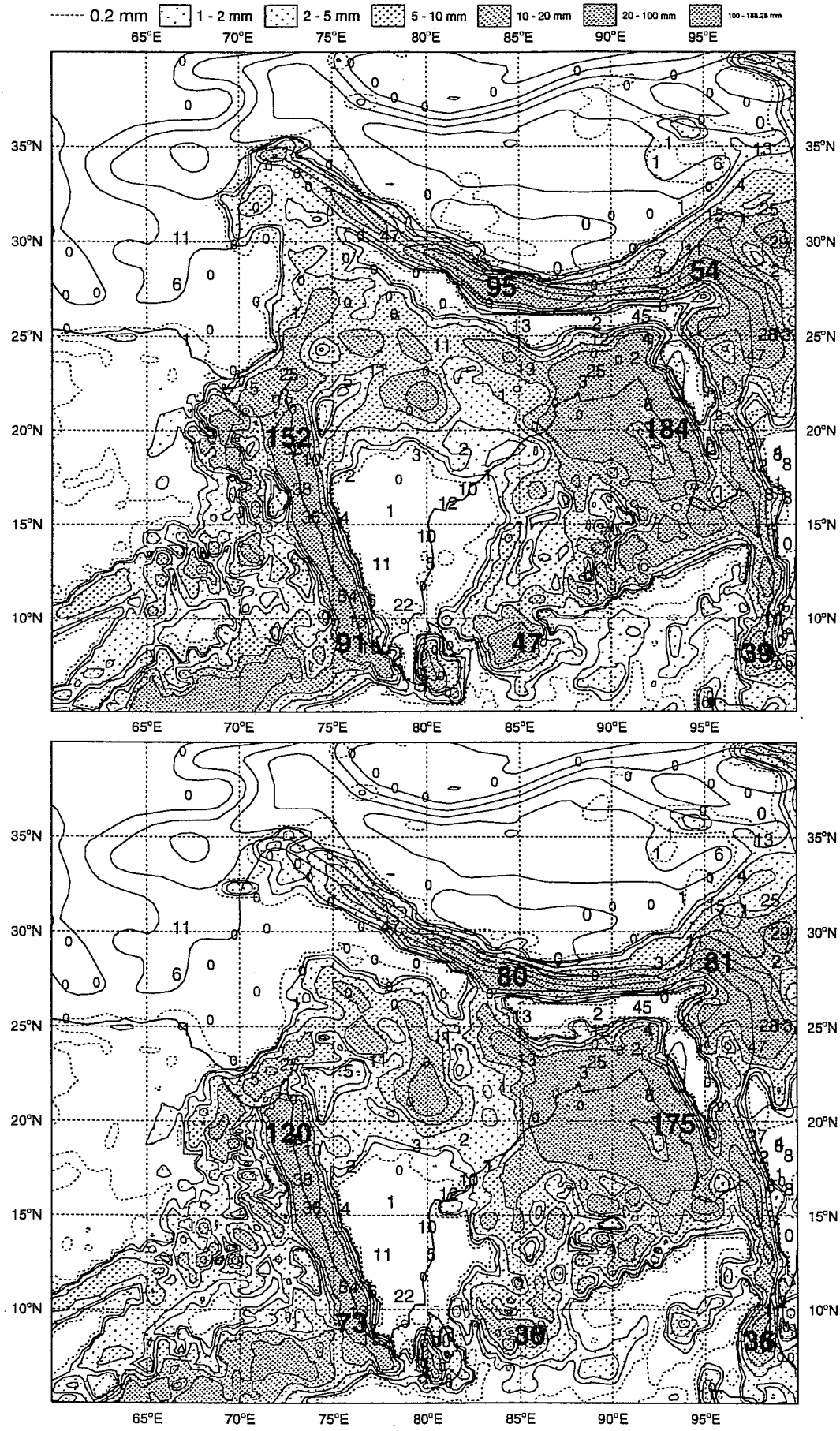

Fig 35 As in Fig 30 but for experiments ZIRC and ZIT6.

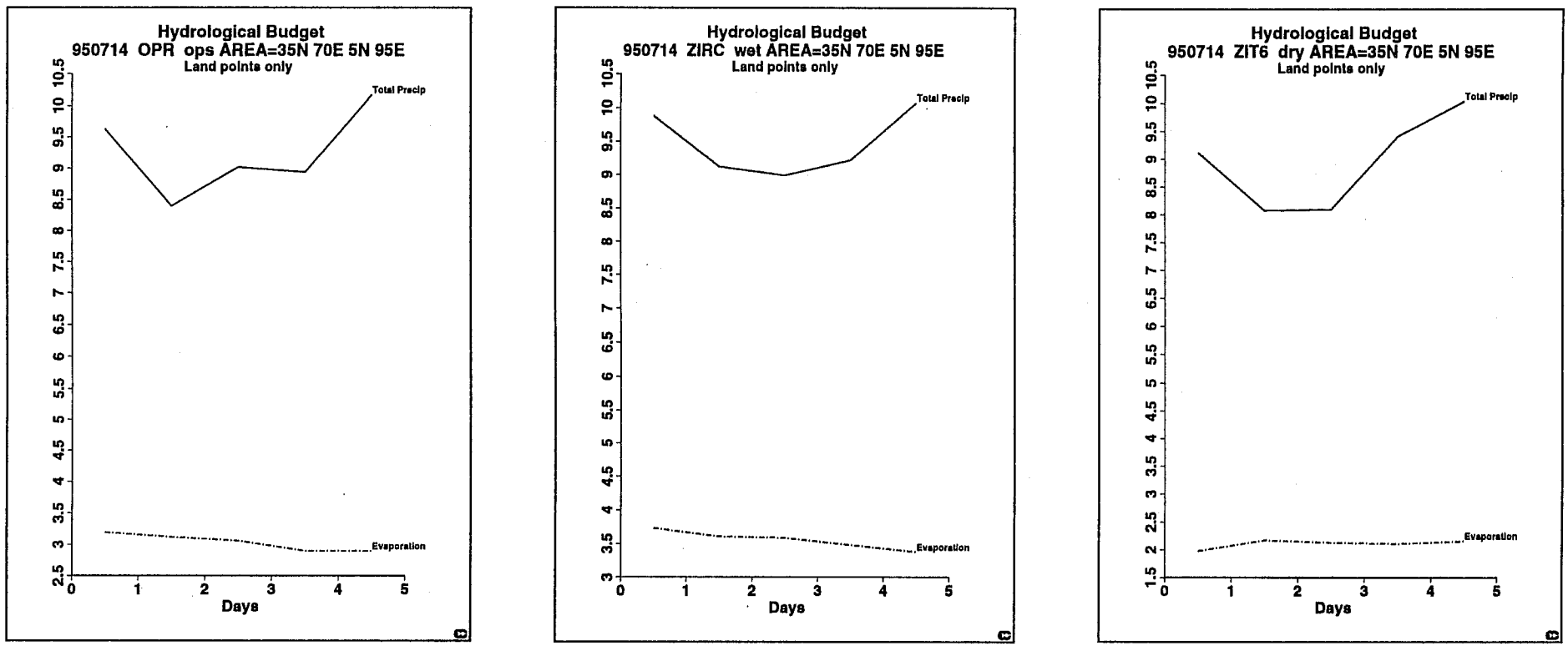

Fig 36 Time series of 5 day forecasts of total precipitation and evaporation averaged over land points of the area 5-35° N, 70-95° E obtained from the initial condition of 14 July, 1995 for OPER, ZIRC and ZIT6.

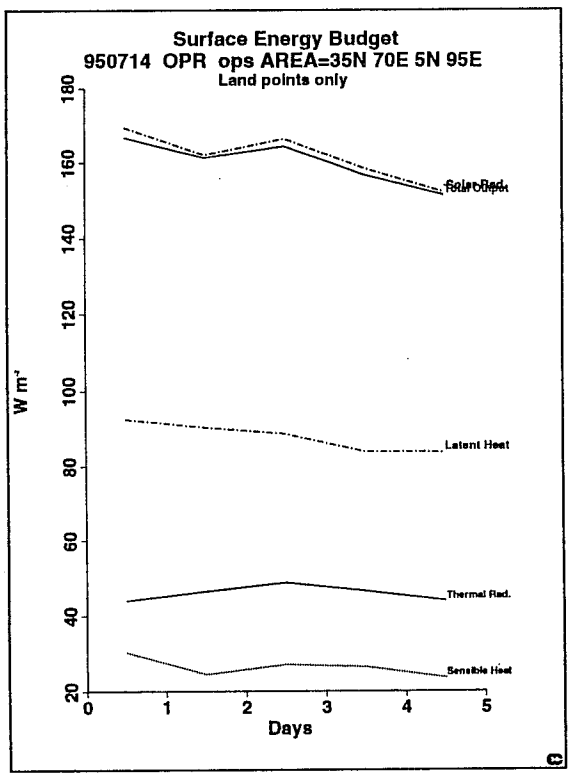

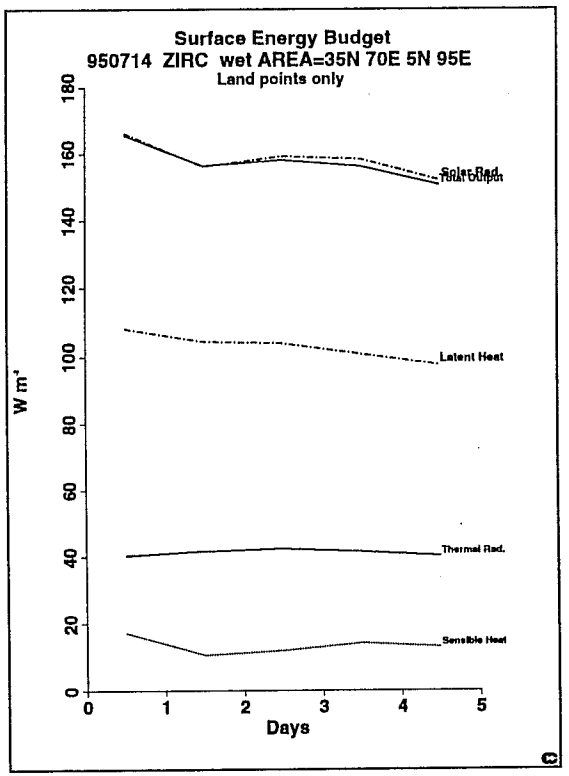

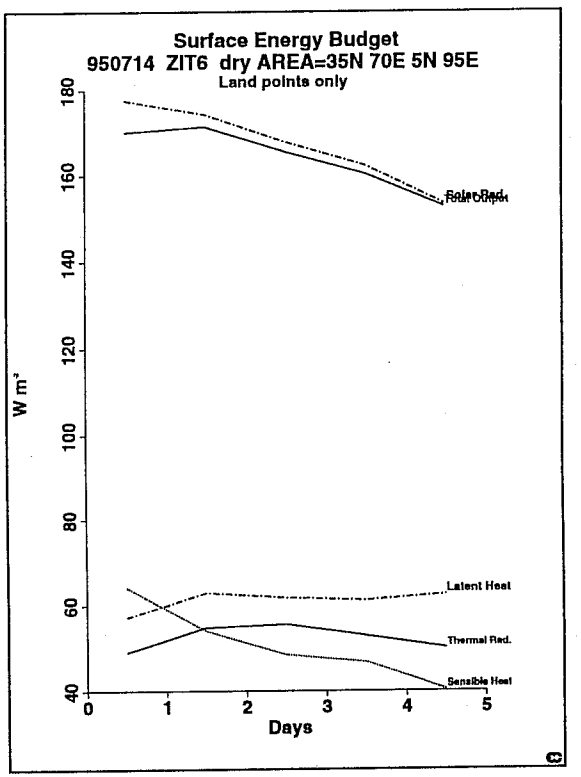

Fig 37 As in Fig 36 but for solar radiation, latent heat, sensible heat, thermal radiation and total output.

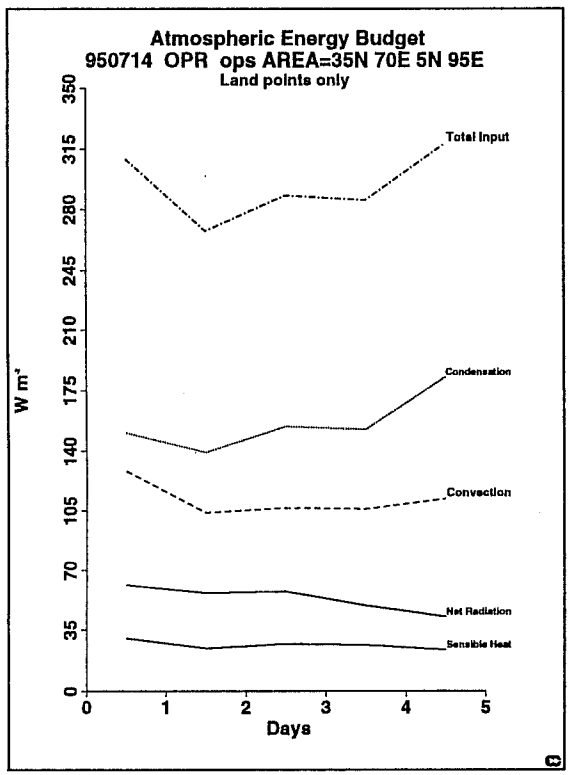

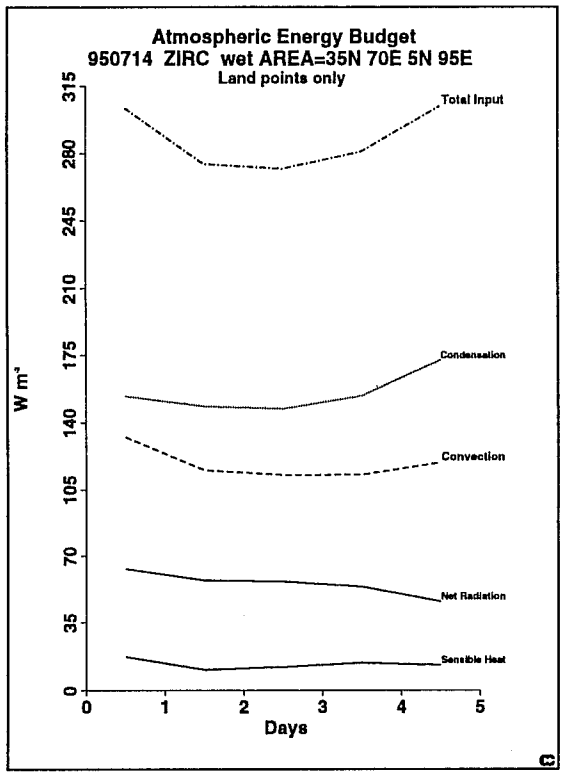

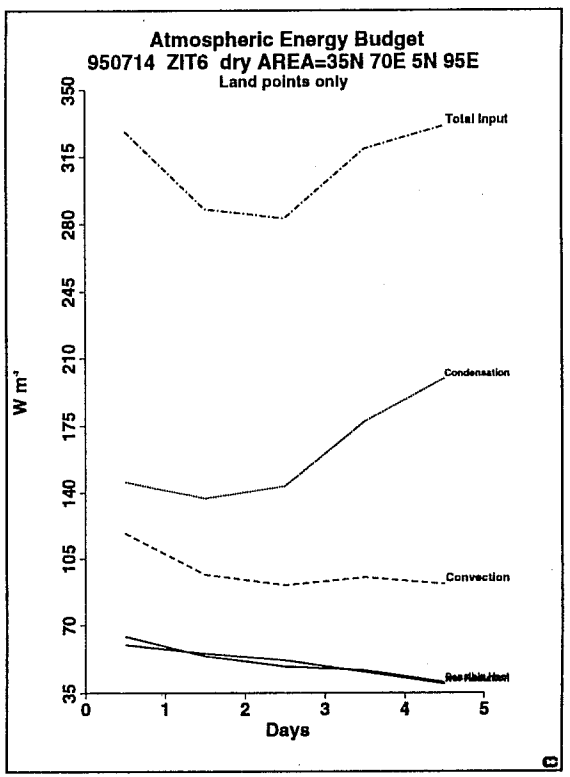

Fig 38 As in Fig 36 but for condensation, convection, net radiation, sensible heat and total output.

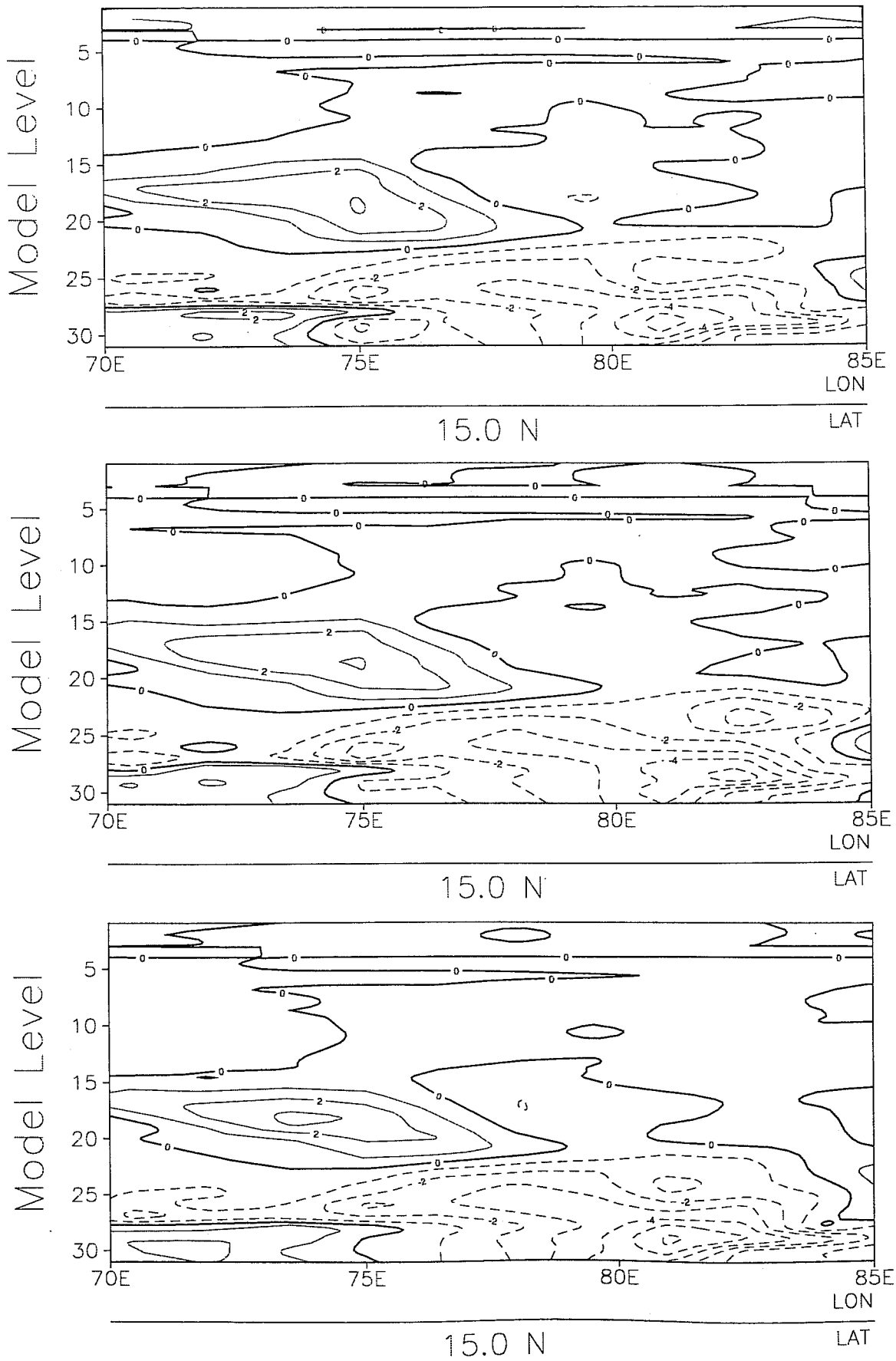

Fig 39 Vertical cross section of the difference between forecast and verifying analysis of specific humidity for 60 hour forecast obtained from the initial for OPER, ZIRC and ZIT6.

rainfall as compared to the old version. This is in contrast to the behaviour over Europe where the rainfall forecasts are clearly better with the new model. The track of cyclonic storm/ monsoon depression were relatively better in the old version. The new model produces better scores of geopotential and wind over the Indian region as compared to the previous version.

Study of the performance during Monsoon-1995 shows a reasonably good simulation of the Somali Jet and cross-equatorial flow during the pre-onset phase. However, the model produced excess upper level easterlies, weak low level westerlies and a relatively strong Hadley cell as compared to the verifying analysis. The onset of the monsoon was predicted about two days in advance as compared to the observed date. However, the model produced relatively weak low level jet and monsoon trough during the active phase. In general, the bias and RMSE of rainfall increased from pre-onset to the onset phase. The model continued to predict better rainfall over Europe and overestimated rainfall over the western Ghat as in the previous year 1994. Quantitatively, the best rainfall forecasts were produced for values less than 0.1 mm/day. It underestimated clouds over northern India during the active phase. Early morning cold bias over northern India was about -9 to -10° C during the pre-onset phase but it improved substantially with the progress of the monsoon when there were more clouds over the region.

Sensitivity experiments were carried out to investigate the problem of underestimation of wide spread convective rainfall over the Indian region. Experiments with the subgrid scale orography were performed to see whether the new model produced excess rainshadow effect on the lee side of the mountain. Results indicated that the operational version produces better simulation of the zones of convergence by allowing the flow to go around the flanks of the mountain and producing less blocking effect. However, the problem of missing rainfall in the forecasts continued. Analysis of results indicated a drying of the lower troposphere in the forecasts. Therefore, two more experiments were carried out by flooding and drying the soil moisture values. Although the problem of rainfall underestimation remained unsolved, the results provided several insights into the physical mechanisms involved. It is argued and anticipated that more investigations of the closure schemes of the convective parametrizations and cloud formulations may lead to the solution of the problem.

ACKNOWLEDGEMENTS

The first author is grateful to NCMRWF for sending him on 5 months deputation to the ECMWF under the UNDP fellowship program and to WMO for providing the financial support. Thanks are due to Drs Adrian Simmons, Anthony Hollingsworth and David Burridge for making his visit possible. We express our thanks to Andreas Lanziger who provided the software to compute the forecast errors for rainfall, cloudiness, 2 metre temperature and the contingency table for threat scores. Many colleagues at ECMWF have provided support at various stages in the completion of this study. The support provided by Christian Jakob, Vesa Karhila, Encarna Serrano, Brian Norris, Bruno David, Dominique Lucas and Norbert Kreitz is gratefully acknowledged.

REFERENCES

Courtier, P and M Naughton, 1994: A pole problem in the reduced Gaussian grid. Q J R Meteorol Soc, **120**, 1389-1407.

Das, P K, 1984: The southwest monsoon. Published by National Book Trust of India.

Das, S, U C Mohanty and O P Sharma, 1987: Semi-Prognostic test of the Arakawa-Schubert cumulus parametrization during different phases of the summer monsoon. Contrib Atmos Phy, **60**, 255-275.

Heymsfield, A J and Leo J Donner, 1990: A scheme for parametrizing ice-cloud water content in general circulation models. J Atmos Sci, **47**, 1865-1877.

Jakob, C, 1994: The impact of the new cloud scheme on ECMWF's integrated forecasting systems (IFS). ECMWF proceedings of the workshop on modelling validation and assimilation of clouds, 1994.

Ju, J and J M Slingo, 1995: the Asian summer monsoon and ENSO. Q J R Meteorol Soc, **121**, 1133-1168.

Krishnamurti, T N, M C Sinha and U C Mohanty, 1995: A study of monsoon energetics. Florida State University, Rep No 95-10.

Lott, F and M Miller, 1995: A new sub-grid scale orographic drag parametrization: its formulation and testing. Submitted to Q J R Meteorol Soc.

Mohanty, U C, R P Pearce and M Tiedtke, 1984: Numerical experiments on the simulation of the 1979 Asian summer monsoon. ECMWF Tech Rep No 44.

Mohanty, U C, J M Slingo and M Tiedtke, 1985: Impact of modified physical processes on the tropical simulation in the ECMWF model. ECMWF Tech Rep No 52.

Morcrette, J-J, 1990: Impact of changes to the radiation transfer parametrization plus cloud optical properties in the ECMWF model. Mon Wea Rev, **118**, 847-873.

Ritchie, H, C Temperton, A Simmons, M Hortal, T Davies, D Dent and M Hamrud, 1995: Implementation of the Semi-Lagrangian method in a high resolution version of the ECMWF forecast model. Mon Wea Rev, **123**, 489-514.

Sundqvist, H, 1988: Parametrization of condensation and associated clouds in models for weather prediction and general circulation simulation. Physically based modelling and simulation of climate and climate change. M E Schlesinger, ed. Kluwer, pp.433-461.

Tiedtke, M, 1989: A comprehensive mass flux scheme for cumulus parametrization in large scale models. Mon Wea Rev, **117**, 1779-1800.

Tiedtke, M, 1993: Representation of clouds in large-scale models. Mon Wea Rev, **121**, No 11, 3040-3061.

Viterbo, P and A C M Beljaars, 1995: An improved land surface parametrization scheme in the ECMWF model and its validation. J Climate, **8**, 2716-2748.

Yanai, M, J H Chu, T E Stark and T Nitta, 1976: Response of deep and shallow tropical maritime cumuli to large scale processes. J Atmos Sci, **33**, 976-991.